Monte Carlo Renormalization Group Study of the SU(3) Lattice Gauge Theory

(Non-perturbative lattice β-function and Perfect action search)

T. Takaishi

Department of Physics, Hiroshima University,

Kagamiyama, Higashi-Hiroshima, 724 Japan

January 13, 1995

Contents

Chapter 1

Introduction

1.1 Problem on Scaling in the Lattice Gauge Theories

In 1974, Wilson[1] has proposed a lattice regularization for Quantum Chromo Dynamics (QCD). The lattice regularization seems the most natural way for analyzing a continuum field theory. This formulation allow us not only a strong coupling expansion but also a Monte Carlo simulation. In particular, the later fascinates people who want to know non-perturbative aspects of QCD. The Monte Carlo simulation for SU(2) lattice gauge theory, first, has been proposed and implemented by Creutz[2] in 1980. Since then, much efforts, improvements of simulation technique and computer developments, have been poured into the Monte Carlo simulation of the lattice gauge theory. Especially it might be worthwhile to remind that physicist's demand on computer went over the supply from the commerce. Some people who are not satisfied with the performance of commercial computers have been starting to construct much faster computers, such as parallel computers[3] and the efforts in this direction are still going on. Recently a typical lattice size for a simulation of pure SU(3) gauge sector (without fermions) has become $24^4 \sim 32^4$ or more[4] owing to developments of computer.

Why do we need to go to such a large lattice? The answer is that we must obtain values of physical quantities in the continuum limit. Mainly observables from the lattice calculations are suffered from two systematic errors[1], the finite lattice spacing and the finite volume effects. Naively we expect that as the lattice size becomes large and the lattice spacing become small we approach to the continuum limit. As for the finite volume effect, it is said that we are already in the region where the finite volume effect is under control by such as an extrapolation to the infinite volume limit[4], and the finite volume effect itself is already small on a lattice currently used in Monte Carlo simulation. On the other hand, the finite lattice spacing effect is still a serious problem.

Now we discuss the finite lattice spacing effect and the scaling violation problem. Let us consider an SU(3) lattice gauge theory. An expectation value of gauge invariant physical quantity Q is defined by Euclidean path integral with respect to gauge field $U_\mu(n)$:

$$< Q >= \frac{1}{Z} \int D[U] Q[U] \exp(-S[U]) \tag{1.1}$$

where $S[U]$ is an action, Z is a normalization factor and $D[U]$ is a Haar measure of SU(3). The standard choice of the action for the SU(3) gauge theory is a simple plaquette Wilson action:

$$S(U) = \beta \sum_{W11} ReTr(1 - W11)/3 \tag{1.2}$$

where $\beta = 6/g^2$ and $W11$ is a plaquette. This action is very popular in the Monte Carlo simulations since it is easy to implement the Monte Carlo simulation on computers. We call this action the *standard Wilson action* from now on and refer to this action if we do not say anything about the form of the action.

In the Monte Carlo simulation, $< Q >$ is evaluated as an average in sequential configuration $\{U = U_1, U_2, U_3, ..., U_N\}$ generated in Markov chain with a proba-

[1]Here we consider a pure gauge theory. In the dynamical case (with fermion), there are two more systematice error, the quenching effect and the finite quark mass effect.

bility distribution:

$$P[U] \propto \exp(-S[U]), \tag{1.3}$$

that is, the important sampled average[5] and a value of $< Q >$ is obtained by:

$$< Q > \simeq \overline{< Q >} = \frac{1}{N} \sum_{i}^{N} Q[U_i]. \tag{1.4}$$

Statistical error of $\overline{< Q >}$ is propotional to $\frac{1}{\sqrt{N}}$. This error can be reduced by sampling a number of $Q[U_i]$. In the limit of $N \longrightarrow \infty$, $\overline{< Q >}$ coincides with $< Q >$. Let us take a physical quantity M with mass dimension as an example. Corresponding to M, Q is constructed of some lattice operators. Q has no dimension and it may be written as:

$$< Q >= m(g) \tag{1.5}$$

where we indicate the coupling g explicitly in order to show the m can be dependent on it. Therefore the m is also given as a non-dimensional quantity and related to the physical observable M with mass dimension by:

$$M(g, a) = \frac{m(g)}{a} \tag{1.6}$$

or alternatively,

$$M(g, a)a = m(g). \tag{1.7}$$

In the lattice gauge theory, scaling means that dimensional physical quantities are independent on the lattice spacing a. This requires that the coupling g should be a function of a and for infinitesimal a it is written as:

$$a\frac{dM(g(a), a)}{da} = 0 \tag{1.8}$$

for all the quantities $M(g(a), a)$ with mass dimension. At finite lattice spacing, however, there is a $O(a^2)$ correction:

$$a\frac{dM(g(a), a)}{da} = O(a^2). \tag{1.9}$$

Assuming e.q.(1.8), we obtain:

$$m - a\frac{\partial g}{\partial a}\frac{\partial m}{\partial g} = 0. \tag{1.10}$$

This equation means that scaling behavior is controlled by the β-function[2] which is defined by:

$$\beta_f(g) = -a\frac{\partial g}{\partial a}. \tag{1.11}$$

Using e.q.(1.11), e.q.(1.10) is rewritten as:

$$m + \beta_f\frac{\partial m}{\partial g} = 0. \tag{1.12}$$

In the perturbative region, the β-function can be expressed by an expansion:

$$\beta_f(g) = -b_0 g^3 - b_1 g^5 + b_2 g^7 + ... \tag{1.13}$$

The first two coefficients, b_0 and b_1 are universal(regularization independent) and well known by the two loop calculation[6]:

$$b_0 = \frac{11N - 2n_f}{3 \times 16\pi^2} \tag{1.14}$$

$$b_1 = \frac{34N^2 - 10Nn_f - 3n_f(N^2-1)/N}{3 \times (16\pi^2)^2} \tag{1.15}$$

where N is the number of colors and n_f is the number of quark flavors. The β-function with the first two terms is called the 2 loop β-function. As we recognize from the definition of the β-function (e.q.(1.11)) the β-function can give us a relation between the coupling g and the lattice spacing a. The important property on the β function is that the coupling g goes to 0 as the lattice spacing a goes to 0 since the coefficient b_0 is positive provided that $11N > 2n_f$. Therefore there is a ultraviolet fixed point at $g = 0$ where the continuum limit of the lattice gauge theory is defined. Taking only the universal first two coefficients, the β function

[2]Do not confuse the coupling β and the β-function. In order to avoid the confusion, we denote β_f for the β-function.

can be easily integrated and the lattice Λ_L parameter with mass dimension is defined as:

$$a(g)\Lambda_L = \exp(-\frac{1}{2b_0 g^2})(b_0 g^2)^{-(\frac{b_1}{2b_0^2})}. \tag{1.16}$$

This tells us the relation between the lattice spacing a and the coupling g. Taking a ratio of e.q.(1.7) and e.q.(1.16), we obtain:

$$\frac{m(g(a))}{a\Lambda_L} = \frac{M(g(a),a)}{\Lambda_L}. \tag{1.17}$$

In the continuum limit, physical quantities should be constant. Hence e.q.(1.17) should also be constant in the continuum limit:

$$\frac{M(g(a),a)}{\Lambda_L} = \frac{M}{\Lambda_L} = constant. \tag{1.18}$$

If e.q.(1.18) holds for all physical quantities, we call it *asymptotic scaling.*

In order to obtain physical quantities in the continuum limit, it is important to establish e.q.(1.18), that is, the asymptotic scaling for all quantities from the lattice Monte Carlo simulation. How can we check the asymptotic scaling? This can be done by analyzing non-perturbatively the β-function on the lattice since the asymptotic scaling is based on the two loop β-function with the first two coefficients in e.q.(1.13) and the β-function calculated non-perturbatively on the lattice can show whether or not the two loop β-function is valid for the region of the coupling β where we are employing the Monte Carlo simulation. Although it is difficult to get the β-function itself directly, it is possible to obtain the β-function in terms of $\Delta\beta$ (this β means the coupling $\beta = 3N/g^2$, for SU(N) gauge theory) which is a coupling shift when the lattice spacing a is changed by some factor. $\Delta\beta$ can give us information of the original β-function. Here we give a relation between $\Delta\beta$ and the two loop β function. Using the definition of the β-function, e.q.(1.13), we integrate:

$$\int_{\beta(a)}^{\beta(a)-\Delta\beta} \frac{dg}{\beta_f(g)} = \int_a^{ba} d\ln a \tag{1.19}$$

where $\beta(a) = 6/g^2(a)$ for SU(3) gauge theory and we take a scale factor b, that is, $a \longrightarrow ba$. Using the 2 loop β-function, we obtain:

$$\Delta\beta_{2Loop} = (\frac{33}{4\pi^2} + \frac{45}{16\pi^4}\frac{1}{\beta}) \ln b \tag{1.20}$$

where we use values of the two loop coefficients for SU(3) gauge theory without fermions, $N = 3$ and $n_f = 0$. E.q.(1.20) is our starting point for analyzing the asymptotic scaling of the SU(3) lattice gauge theory. Comparisons between $\Delta\beta_{2Loop}$ of e.q.(1.20) and $\Delta\beta$ from the lattice study tell us whether or not we are in the asymptotic scaling region.

There are two popular methods to analyze $\Delta\beta$, the ratio method[7] and the operator matching method by the Monte Carlo Renormalization Group (MCRG) technique[24]. The ratio method is based on the fact that the ratio of Wilson loops:

$$R(i,j,k,l) = \frac{W(i,j)}{W(k,l)} \tag{1.21}$$

satisfies an approximate homogeneous renormalization group equation:

$$R(2i,2j,2k,2l,g(a),2L) = R(i,j,k,l,g(2a),L) \tag{1.22}$$

where $i + j = k + l$. Using values of Wilson loops from the Monte Carlo simulation on 2 lattices of size $2L$ and L, the couplings $g(2a)$ and $g(a)$ which satisfies e.q.(1.22) is searched out. This gives us $\Delta\beta$ we want as:

$$\Delta\beta = \frac{6}{g^2(a)} - \frac{6}{g^2(2a)} \tag{1.23}$$

Due to the lattice artifacts, however, e.q.(1.22) is exact for Wilson loops of infinite size, that is, $i, j, k, l \rightarrow \infty$. Therefore in order to obtain reliable results of $\Delta\beta$, one has to prove the convergence of the value of $\Delta\beta$ as a function of loop size. However measurements of large Wilson loops are practically difficult since we need a large lattice and much statistics. Moreover it is known that from SU(2) Monte Carlo simulations, the convergence with respect to loop size is very slow.

On the other hand, the operator matching method by the MCRG technique seems to be more efficient. There are two main groups who have analyzed $\Delta\beta$ using the MCRG technique. Bowler *et al.*[8] have obtained $\Delta\beta$ up to $\beta = 6.6$ on 16^4 lattices using the MCRG with a scale factor 2 blocking. They have reconfirmed that there is a pronounced dip around $\beta = 6.0$ which has already observed in the study by the ratio method[7] and showed that $\Delta\beta$ approaches to the prediction of the 2 loop β-function as β increases and reaches it at $\beta = 6.6$. In their further research[9], however, they have observed the difference from the prediction of the 2 loop β-function at higher β, 6.9 and 7.2. On the other hand, Gupta *et al.*[10, 11] analyzed $\Delta\beta$ on 9^4 lattices up to $\beta = 7.5$ and they have claimed that $\Delta\beta$ reaches the prediction of the 2 loop β-function already at $\beta = 6.75$, and concluded that there is the asymptotic scaling above $\beta = 6.75$. Those results are plotted in Fig.1. The results from $b = \sqrt{3}$ blocking are rescaled to $b = 2$ blocking according to e.q.(1.20) although this rescale procedure is not accurate if the results are not in the asymptotic scaling region. Hoek[12] have also analyzed $\Delta\beta$ using the MCRG technique and he has found the slow approach to the asymptotic scaling region using phenomenological fit to the β-function[13]. This is a controversy and we can not conclude from these results of $\Delta\beta$ where the asymptotic scaling is. Chapter 2 is devoted to solve this controversy. We carry out the MCRG study with a scale factor 2 blocking on both 16^4 and 32^4 lattices. A feature of our study is that we use a large lattice, a 32^4 one and do high statistics Monte Carlo simulations. Typically we update gauge configurations 20,000-100,000 sweeps and measure observables every 10th sweep. Therefore We have 2,000-10,000 configurations. This statistics is much higher than others (They have used about 100 configurations.). We consider that the controversy comes from 2 effects, the finite temperature phase transition and the poor matching condition. On a small lattice the lattice system goes through the finite temperature phase transition as β increases, for example at $\beta \simeq 6.4$ on a 16^4 lattice. The finite temperature phase transition causes the difficulty of determination of $\Delta\beta$. If we employ the work on a 32^4 lattice, we

remain in the confinement region up to $\beta \simeq 7.0$. This is one of advantages of using a 32^4 lattice. The second advantage is that on a large lattice we can make the matching condition better since for instance on a 32^4 lattice we can do the scale factor 2 blocking one more time than on a 16^4 lattice and this ensures that the blocked trajectory approaches to the renormalized trajectory more.

The analysis of $\Delta\beta$ using the MCRG technique is a main theme in Chapter 2 and we solve the controversy and discuss the scaling behavior[14, 15, 16, 17, 18, 19, 20, 21, 22].

1.2 Perfect Action

As we will see later in Chapter 2, the standard Wilson action has a poor scaling property. This can not be completely compensated with some remedies such as improved couplings. Do we need to go to higher β and a larger lattice in order to confirm the scaling? The answer is not necessarily YES. We have another way, improvements of actions. The standard Wilson action is widely used in the current Mont Carlo simulations because of its simplicity. We can choose other actions in such a way that the the cut-off dependence near the continuum limit decreases. Such a systematic procedure to improve the action has been proposed by Symanzik[23]. Let us see Symanzik's improvement program briefly. The standard Wilson action has $O(a^2)$ correction to the continuum action in the vicinity of the continuum limit. E.q.(1.2) has a form in the limit of the lattice spacing a goes to 0:

$$S(U) = \frac{a^4}{2} \sum_{n,\mu,\nu} Tr(F_{\mu\nu}^2(n)) + O(a^6). \tag{1.24}$$

$O(a^6)$ terms and other higher power of a terms disappear in the continuum limit. However $O(a^6)$ terms can be removed out of the continuum limit by adding 6 link loop terms. Hence it is considered that such an action for which $O(a^6)$ terms are removed approaches to the continuum limit fast. The action including 6 link

loop terms is written as:

$$S(U)_6 = \sum_{W11} c_0 Tr(1 - W11) + \sum_{W12} c_1(1 - W12) + \sum_{Wchair} c_2(1 - Wchair) + \sum_{Wtwist} c_3(1 - Wtwist) \tag{1.25}$$

where shapes of 6 link loops are displayed in Fig.2. After some calculations, we have the following:

$$\begin{aligned} S(U)_6 &= -\frac{a^4}{2}(c_0 + 8c_1 + 16c_2 + 8c_3) \sum_{n,\mu,\nu} Tr(F_{\mu\nu}^2(n)) \\ &+ a^6(c_2 + \frac{c_3}{3}) \sum_{n,\mu,\nu,\lambda} Tr(D_\mu F_{\mu\lambda}(n) D_\nu F_{\nu\lambda}(n)) \\ &+ \frac{a^6}{12}(c_0 + 20c_1 + 4c_2 - 4c_3) \sum_{n,\mu,\nu} Tr(D_\mu F_{\mu\nu}(n))^2 \\ &+ a^6 \frac{c_3}{3} \sum_{n,\mu,\nu,\lambda} Tr((D_\mu F_{\nu\lambda}(n))^2) + O(a^8) \end{aligned} \tag{1.26}$$

The conditions to remove $O(a^6)$ terms are:

$$c_0 + 8c_1 + 16c_2 + 8c_3 = 1 \tag{1.27}$$

$$c_0 + 20c_1 + 4c_2 - 4c_3 = 0 \tag{1.28}$$

$$c_2 = c_3 = 0. \tag{1.29}$$

From these conditions, we have coefficients for the so-called Symanzik improved action:

$$c_0 = \frac{5}{3} \tag{1.30}$$

$$c_1 = -\frac{1}{12} \tag{1.31}$$

and $c_2 = c_3 = 0$.

Other improved actions have been proposed by Wilson[24] and Iwasaki[25]. They have determined coefficients of 6 link loop action using the blocking transformation. The coefficients they have obtained are:

$$c_0 = 4.376 \tag{1.32}$$

$$c_1 = -0.252 \tag{1.33}$$

$$c_2 = 0 \tag{1.34}$$

$$c_3 = -0.17 \tag{1.35}$$

for Wilson's improved action for the SU(2) gauge theory and

$$c_1 = -0.331 \tag{1.36}$$

$$c_0 = 1 - 8c_1 \tag{1.37}$$

$$c_2 = c_3 = 0 \tag{1.38}$$

for Iwasaki's improved action for the SU(3) gauge theory. Using these improved actions some Monte Carlo simulations have been performed but drastic improvements have not been fulfilled yet[26, 27, 28].

Recently other program to improve the action has been advocated by P.Hasenfratz and Neidermayer[29]. They have determined the classical perfect action[3] (or fixed point action) by solving the saddle point equation for $O(3)$ non-linear σ model. The continuum limit is defined on the critical surface (the correlation length is infinity). The continuum limit means that there is no lattice artifact and the continuum physics is obtained there. There is a fixed point on the critical surface. At the fixed point, the form of the action S^* is unchanged by the Renormalization Group transformation:

$$S^* = RS^* \tag{1.39}$$

where R indicates the operation of the Renormalization Group transformation. There is a one dimensional flow, the Renormalized trajectory, which flows from the fixed point according to the Renormalization Group transformation. On the Renormalized trajectory, there is also no lattice artifact. They approximated the Renormalization trajectory with the fixed point action $\beta_1 S^*$(See Fig.3).

This program successfully works for $O(3)$ non-linear σ model and restoration of the rotational invariance is shown. The program on SU(3) gauge theory is also

[3]The perfect action means that its action is completely free from lattice artifacts.

going on[30]. However the action obtained by such a program is not a complete perfect action. Even if we get a classical perfect action, it is not insured that the action works at moderate finite coupling since the renormalization effects are non-trivially dependent on the blocking scheme at finite β(See Fig.3). Namely at moderate finite coupling, the approximation of the fixed point action is not enough.

The MCRG technique can be used for the perfect action search since the blocked trajectory goes to the renormalized trajectory and flows along the renormalized trajectory lastly. In principle, if we can obtain an effective action after enough blocking steps, it will be one of perfect actions. However it was very difficult to obtain such an effective action since we did not have a practical method to obtain it. Recently, however, quite an efficient method, the canonical demon method, has been proposed and applied for $O(3)$ non-linear σ model[51]. It has been shown that the method works well for $O(3)$ non-linear σ model. In Chapter 3, we report an application for physically interesting case, SU(3) gauge theory and try to obtain an effective action on blocked configurations[52].

Chapter 2

MCRG Analysis of the lattice β-function

2.1 Monte Carlo Renormalization Group

The idea of the Monte Carlo Renormalization Group (MCRG), which combines the Renormalization Group with the Monte Carlo simulation, first, was given by Ma[31] and developed by Swendsen[32] in spin systems and by Wilson[24] in lattice gauge theories. In the vicinity of the critical point, the correlation length diverges and all the length of scales contribute the dynamics of the system. In other words, infinitely many degrees of freedom arise in the system. The standard Monte Carlo simulations face with hard problems at or near critical point. The physical size of the system, in Monte Carlo simulations, should be larger than the correlation length, at least a few times, in order to obtain meaningful results. As we approach to the critical point, computer time used for the Monte Carlo simulation increases inevitablely since a large lattice is needed to keep size of the system larger than the correlation length. There also exits the critical slowing down problem which makes the Monte Carlo simulation much difficult.

The Renormalization Group method sheds light for us to handle the problems in the vicinity of the critical point. General concepts of the Renormalization

Group is an integration over the irrelevant degrees of freedom keeping those which are relevant for physical quantities of the system. In the MCRG technique, the Renormalization Group transformation is performed for configurations generated by the Monte Carlo simulation[31]. To illustrate what the MCRG is like, let us consider the 2-dimensional Ising system which described by a Hamiltonian:

$$H = -K_1 \sum_{<i,j>} s_i s_j \tag{2.1}$$

where spin s_i takes ± 1 and $< i, j >$ means that the summation is taken for the nearest neighbor pairs. The partition function of the system is written as:

$$Z = \sum e^{-H} = \sum_{S_1} e^{K_1 S_1} \tag{2.2}$$

where we use the brief expression, $S_1 = \sum_{<i,j>} s_i s_j$, and configurations are generated with the probability distribution:

$$P(S_1) \propto e^{K_1 S_1}. \tag{2.3}$$

The Renormalization Group transformation acts on spin configuration s_i and transforms them to new transformed spin configuration s'_i. The transformation procedure is often called *blocking*. Let us take a scale factor 2 blocking. Spins in a block α are mapped onto ± 1 according to a transformation rule, such as majority rule(See Fig.4). This procedure is symbolically written as:

$$s'_\alpha = f(s_i) \tag{2.4}$$

where $i \in$ block α. The probability of observing a new configuration $[s'_\alpha]$ is proportional to $\exp(-H'[s'_\alpha])$ which is written as:

$$e^{-H'[s'_\alpha]} = \sum_{[s_i]} \prod_\alpha \delta(s'_\alpha - f(s_i)|_{i\in\alpha}) e^{-H[s_i]}. \tag{2.5}$$

After the blocking, the Renormalization Group transformation may produces many couplings. Hence the form of H' can be complicated. For instance, we can

generalize the Hamiltonian H' by writing:

$$-H' = K_1 \sum_{<i,j>} s_i s_j + K_2 \sum_{<<i,j>>} s_i s_j + K_s \sum_{i,j,k,l} s_i s_j s_k s_l + ... \quad (2.6)$$

$$= K_1 S_1 + K_2 S_2 + K_3 S_3 + ... \quad (2.7)$$

where S_1, S_2 and S_3 are

$$S_1 = \sum_{<i,j>} s_i s_j \quad (2.8)$$

$$S_2 = \sum_{<<i,j>>} s_i s_j \quad (2.9)$$

$$S_3 = \sum_{i,j,k,l} s_i s_j s_k s_l \quad (2.10)$$

and $<< i,j >>$ the next-to-nearest neighbor pair and i,j,k,l is the plaquette interaction pair.

Note that the partition function of the transformed system equals that of the initial system provided that the Kadanoff constraint is satisfied:

$$\sum_{[s'_\alpha]} \prod_{\alpha} \delta(s'_\alpha - f(s_i)|_{i\in\alpha}) = 1. \quad (2.11)$$

Using this condition, it is easily checked that:

$$Z = \sum_{[s_i]} e^{-H[s_i]} = \sum_{[s'_i]} e^{-H[s'_i]} = Z' \quad (2.12)$$

It is also considered that the Renormalization Group transformation acts on coupling space.

$$K'_\alpha = R_{\alpha\beta} K_\beta \quad (2.13)$$

where $R_{\alpha\beta}$ is a transformation matrix of the couplings. Let us denote the coupling at the fixed point K^*_α. At the fixed point, K^*_α is not changed as:

$$K^{*\prime}_\alpha = R_{\alpha\beta} K^*_\beta = K^*_\alpha \quad (2.14)$$

In the vicinity of the fixed point, the coupling K_α is expressed by:

$$K_\alpha = K^*_\alpha + \delta K_\alpha. \quad (2.15)$$

Therefore we obtain:

$$K'_\alpha = K^*_\alpha + \delta K'_\alpha \tag{2.16}$$

$$= K^*_\alpha + R_{\alpha\beta}\delta K_\beta \tag{2.17}$$

where the transformation matrix is:

$$R_{\alpha\beta} = \frac{\partial K'_\alpha}{\partial K_\beta}|_{K^*}. \tag{2.18}$$

Generalizing e.q.(2.18) to n-th blocking, we obtain:

$$R^n_{\alpha\beta} = \frac{\partial {K_\alpha}^n}{\partial K^{n-1}_\beta}|_{K^*} \tag{2.19}$$

$$= \frac{\partial {K_\alpha}^n}{\partial < S^n_\alpha >} \frac{\partial < S^n_\alpha >}{\partial {K_\beta}^{n-1}}. \tag{2.20}$$

This can be calculated using the following identities[32]:

$$\frac{\partial < S^n_\alpha >}{\partial K^{n-1}_\alpha} = < S^n_\alpha S^{n-1}_\beta > - < S^n_\alpha >< S^{n-1}_\beta > \tag{2.21}$$

$$\frac{\partial < S^n_\alpha >}{\partial K^n_\alpha} = < S^n_\alpha S^n_\beta > - < S^n_\alpha >< S^n_\beta > \tag{2.22}$$

where $< S^n_\alpha >$ are the expectation values on the n-th blocked lattice. The critical exponent ν is obtained by the leading eigenvalue λ of $R_{\alpha\beta}$:

$$\nu = \frac{\ln b}{\ln \lambda} \tag{2.23}$$

where b is the scale factor of the blocking.

In the lattice gauge theory, blocking is somehow complicated since the variable is defined on the link. The blocked link is constructed from a sum of paths:

$$X = \sum path \tag{2.24}$$

In general, this sum is not an SU(N) matrix and the new blocked link is selected with the probability distribution:

$$P(U_b) \propto \exp(pTrU_bX) \tag{2.25}$$

where p is a parameter to optimize the blocking.

Several ways to construct the paths of e.q.(2.24) have been proposed since there is no unique blocking. Wilson[24] has proposed a scale facto $b = 2$ blocking whose geometry of the blocking is shown in Fig.5. 8 links are summed up(in Fig.5 only 4 of 8 links are shown in 3-dimension.). This blocking requires the gauge fixing since the end of links are not connected. The gauge fixing procedure is very costly in the Monte Carlo simulations. Hence this blocking transformation has not been pursued since Wilson proposed and tried to obtain values of $\Delta\beta$. Swendsen[33] has proposed the gauge invariant scale factor $b = 2$ blocking, which does not require the gauge fixing. In this blocking step, paths which connects 2 sites are summed up(Fig.6). Therefore all the paths are connected at the blocked sites. Other blockings with a different scale factor, based on Swendsen blocking, have also been proposed, scale factor $b = \sqrt{3}$[34] and $b = \sqrt{2}$[35]. These are specific to the gauge theories in 4-dimension.

2.2 Blocking Transformation

We follow Swendsen's scale factor 2 blocking[33]. The blocking procedure we take is as follows: Path ordered links connecting two lattice sites separated with two lattice spacings are summed up(Fig.6):

$$Q_\mu(n) = aU_\mu(n)U_\mu(n+\mu) + b\sum_{\nu\neq\mu} U_\nu(n)U_\mu(n+\nu)U_\mu(n+\mu+\nu)U_\nu^\dagger(n+2\mu) \quad (2.26)$$

where we take $a = 1$ and $b = 1/2$. The matrix $Q_\mu(n)$ is not an SU(3) matrix. So we have to extract an SU(3) matrix from it. In the case of SU(2) gauge theory, such a sum is in proportion to an SU(2) matrix because of the speciality of SU(2) matrix. Therefore it can be easily normalized to an SU(2) matrix. On the other hand, the SU(3) matrix does not have such property. We have to employ other procedure to project a non-SU(3) matrix onto one of SU(3) group. We define such a projection by a maximization of a function $ReTr(Q_\mu(n)P_\mu^\dagger(n))$, where an

SU(3) matrix $P_\mu(n)$ is taken so that $ReTr(Q_\mu(n)P_\mu^\dagger(n))$ takes a maximum:

$$P_\mu(n) \longleftarrow \max[ReTr(Q_\mu(n)P_\mu^\dagger(n))]. \tag{2.27}$$

This definition preserves local gauge invariance. The maximization can be done by the polar decomposition[36, 10, 11]. In the polar decomposition step, $Q_\mu(n)$ is decomposed as:

$$Q_\mu(n) = HVDe^{i\phi}V^\dagger \tag{2.28}$$

where D is a positive definite diagonal matrix and H and V are SU(3) matrixes. Using this decomposition, we can maximize:

$$ReTr(De^{-i\phi}X) \tag{2.29}$$

where X is given by:

$$X = V^\dagger H^\dagger PV. \tag{2.30}$$

In the polar decomposition, H is given by:

$$H = Q_\mu(n)(Q_\mu^\dagger(n)Q_\mu(n))^{\frac{-1}{2}}e^{-i\alpha/3}. \tag{2.31}$$

where $\alpha = arg(det(Q_\mu(n)))$. It is known that for $\beta > 6.0$ the phase ϕ is approximately 0 and H and P are approximately same. At $\beta = 6.0$ the difference between H and P by comparing average values of Wilson loops is already small (about $1 \approx 2\%$) and the difference decreases as β increases. Therefore we use H as an SU(3) matrix mapped from $Q_\mu(n)$, that is, $P_\mu(n) = H$.

We introduce a parameter q in order to optimize the blocking. The meaning of the optimization will be clarified later. A blocked link $U_\mu^{(b)}(n)$ is given as a product of $P_\mu(n)$ and a random gaussian SU(3) matrix:

$$U_\mu^{(b)}(n) = P_\mu(n)U_{random\_gauss} \tag{2.32}$$

$$= HU_{random\_gauss}. \tag{2.33}$$

The random gaussian SU(3) matrix is given by:

$$U_{random\_gauss} = \exp\left(i\sum_{i=1}^{8}\frac{c_i\lambda_i}{2}\right) \tag{2.34}$$

where λ_i, $i = 1, ..., 8$ are SU(3) generators and the c_i are real numbers generated with the distribution:

$$\rho(c_i) \propto \exp(\frac{c_i^2}{2q}). \tag{2.35}$$

In our Monte Carlo simulations, the blocking is repeatedly performed until the size of the lattice becomes 2^2.

Our blocking scheme is also written in the form of e.q.(2.5) (See Appendix A):

$$\begin{aligned} \exp(-S'[U']) &= \int [dU] exp(-S[U] + N(Q) \\ &\quad + p \sum_n ReTr(U_\mu^{(b)}(Q_\mu^\dagger(n)Q_\mu(n))^{\frac{-1}{2}} e^{-i\alpha/3} Q_\mu^\dagger(n)) \end{aligned} \tag{2.36}$$

where

$$p = \frac{2}{q} - \frac{1}{2} \tag{2.37}$$

$$det[Q_\mu(n)] = r \exp(i\alpha) \tag{2.38}$$

and the normalization factor $N(Q)$ is:

$$N(Q) = \sum_{n,\mu} - \ln[\exp(3(\frac{2}{q} - \frac{1}{2})(2q\pi)^4]. \tag{2.39}$$

2.3 Matching Method

2.3.1 Definition of $\Delta\beta$

Here we give a definition of $\Delta\beta$. $\Delta\beta$ is defined as a coupling shift when the lattice spacing a is changed to $2 \times a$:

$$\Delta\beta = \Delta\beta(\beta(a)) = \beta(a) - \beta(2a) \tag{2.40}$$

where a is a lattice spacing and $\beta(a) = 1/g^2(a)$.

Inversely we can consider the lattice spacing as a function of the coupling β. Starting from a coupling β, we search a coupling β' which satisfies:

$$2a(\beta) = a(\beta'). \tag{2.41}$$

$\Delta\beta$ is obtained by:

$$\Delta\beta(\beta) = \beta - \beta'. \tag{2.42}$$

2.3.2 $\Delta\beta$ from Matching Method

How can we obtain a value of $\Delta\beta$ in the blocking? We can utilize the operator matching (or two lattice matching) method in order to obtain $\Delta\beta$. This method has been originally advocated by Wilson[24] and he tried to obtain $\Delta\beta$ on rather small lattices, 8^8 ones.

To see what the operator matching method is, let us do the blocking n times. After n-th blocking step, the lattice spacing becomes 2^n times bigger than the one on the initial lattice. The lattice spacing can be written as:

$$a^{(n)}(\beta) = 2^n a(\beta) \tag{2.43}$$

where β indicates that the blocking is done on the configuration generated at $\beta = \frac{6}{g^2}$. We would like to find β' which satisfies e.q.(2.41). In order to obtain a recipe to find β', first let us assume that e.q.(2.41) is satisfied and do the blocking $(n-1)$ times at β'. We obtain a relation:

$$a^{(n-1)}(\beta') = 2^{n-1} a(\beta'). \tag{2.44}$$

Using e.q.(2.41) and e.q.(2.43) we find the following relation:

$$a^{(n-1)}(\beta') = 2^n a(\beta) = a^{(n)}(\beta) \tag{2.45}$$

This equation is telling us that β' can be determined by searching a value of the coupling at which the lattice spacing after $(n-1)$-th blocking step coincide with the one after n-th blocking step at β. Here we can ask ourselves "How can we recognize such a coincidence of the lattice spacing in e.q.(2.45)?". It is not so easy to find the coincidence by directly measuring the lattice spacing a. Fortunately the operator matching method can give us a criterion of the coincidence. Therefore we follow the operator matching method and hereafter we call it simply the matching method.

Let us assume that after n-th blocking step, the blocked trajectory reaches the renormalized trajectory completely(See also Fig.7). We define a value of Wilson loop operator O_k there as:

$$O_k = O_k(a^{(n)}(\beta)). \tag{2.46}$$

In terms of the operator, e.q.(2.45) means:

$$O_k(a^n(\beta)) = O_k(a^{(n-1)}(\beta'_k)). \tag{2.47}$$

In e.q.(2.47) we put the suffix k on β' in order to indicate that we are searching β' for each Wilson loop operator. However if both of the blocked trajectories from β and β'_k are already on the renormalized trajectory, a value of each β'_k should be the same value. Namely for all the Wilson loops the next equation holds:

$$O_k(a^n(\beta)) = O_k(a^{(n-1)}(\beta')). \tag{2.48}$$

Therefore β' can be obtained by comparing values of Wilson loops on n-th blocked lattice and on $(n-1)$-th blocked one, and searching β' which matches e.q.(2.48). This is the reason that the method is called operator matching method. The measurements of Wilson loop should be done on a lattice with the same physical volume to avoid the finite volume effect since we are employing on the finite lattice. This means that when $O_k(a^{(n)}(\beta))$ is measured on a blocked lattice from a N^4 lattice, $O_i(a^{(n-1)}(\beta'_i))$ should be measured on a blocked lattice from a $(N/2)^4$ lattice in order to keep the physical volume same.

So far we have assumed that the blocked trajectory after n-th blocking step already reaches the renormalized trajectory. If not the case, e.q.(2.48) does not hold for all the Wilson loops. Hence $\Delta\beta$ which we obtain from each Wilson loop does not give us the same value. How can we make sure that the blocked trajectory are on the renormalized trajectory? It is not obvious that how many blocking step we should do in order to reach the renormalized trajectory. It completely depends on what blocking scheme we take. However even if we take a slow blocking scheme(bad blocking scheme), enough many blocking steps can lead

the blocking flow to the renormalized trajectory since it is fated that the blocked trajectory becomes to flow along the renormalized trajectory lastly. Therefore to do many blocking steps is an advantage in a sense of reaching the renormalized trajectory and making sure that we are on the renormalized trajectory. This is one of reasons why we use a 32^4 lattice twice bigger than a 16^4 lattice as mentioned briefly in Sec.1.1. We can do the blocking one more time.

There is a freedom to optimaize the blocking in such a way that the blocked trajectory reaches the renormalized trajectory fast. Actually, it is very important to take such an optimal blocking scheme since the number of blocking step we can do is limited within a few blocking steps. In Sec.2.2 we have introduced the q parameter in the blocking transformation. This parameter can be tuned so that the blocked trajectory reaches the renormalized trajectory fast. In principle, we can find a value of the optimal parameter changing a value of q continuously in a Monte Carlo run. However such a process to find the optimal parameter is very costly. In practice we can employ at most at several q points.

Fortunately dependence of $\Delta\beta_k$ on q is moderate and we can approximate it by a linear function in terms of q:

$$f_k(q) = \Delta\beta_k(q) = d_1 q + d_2. \tag{2.49}$$

In the Monte Carlo run, as mentioned above, we run at several q points ($q_l = q_0$, q_1, q_3, ...). Hence we obtain $\Delta\beta_k(q_l) \pm \delta\Delta\beta_k(q_l)$ for q_l, where $\delta\Delta\beta_k(q_l)$ is an error of $\Delta\beta_k(q_l)$. Using this set, e.q.(2.49) is obtained by a fitting. Note that the criterion that we are on the renormalized trajectory is that for all the Wilson loops we obtain the same value of $\Delta\beta$. Therefore we can define the optimal q parameter where all $f_k(q)$ intersect each other. Our procedure to find the optimal q parameter is as follows:

An error of the fitted line is defined as:

$$\delta f_k(q) = \sum_l \left(\frac{\partial f_k(q)}{\partial \Delta\beta_k(q_l)} \right)^2 (\delta\Delta\beta_k(q_l))^2. \tag{2.50}$$

The optimal value of q $(= q_{opt})$ is defined at the best intersection point where the function $S(q)$ takes a minimum:

$$S(q_{opt}) = \min S(q), \tag{2.51}$$

$$S(q) = \sum_k \frac{(\bar{f}(q) - f_k(q))^2}{\delta f_k(q)^2} \tag{2.52}$$

where $\bar{f}(q)$ is an average of all the $f_k(q)$ at q, which is defined by:

$$\bar{f}(q) = \sum_k \frac{f_k(q)}{\delta f_k(q)^2} / \sum_k \frac{1}{\delta f_k(q)^2}. \tag{2.53}$$

Using q_{opt}, we obtain $\Delta\beta$ as:

$$\Delta\beta = \bar{f}(q_{opt}). \tag{2.54}$$

In order to know accuracy of obtained $\Delta\beta$, we define the error of $\Delta\beta$ as follows: First we define an error of q_{opt} as:

$$\delta q_{opt}^2 = \sum_{k,l} \left(\frac{\partial q_{opt}}{\partial \Delta\beta_k(q_l)} \right)^2 (\delta\Delta\beta_k(q_l))^2. \tag{2.55}$$

Here the derivative in e.q.(2.55) can be evaluated by a numerical calculation. Using e.q.(2.55), the error of $\Delta\beta$ is defined by:

$$\delta\Delta\beta = \frac{1}{2} \left| \bar{f}(q_{opt} + \delta q_{opt}) - \bar{f}(q_{opt} - \delta q_{opt}) \right|. \tag{2.56}$$

Alternatively $\Delta\beta$ can be considered as a function of the $\Delta\beta_k(q_l)$. Therefore the error of $\Delta\beta$ is also defined as:

$$\delta\Delta\beta = \sum_{k,l} \left(\frac{\partial \Delta\beta}{\partial \Delta\beta_k(q_l)} \right)^2 \delta\Delta\beta_k(q_l)^2. \tag{2.57}$$

The derivatives in e.q.(2.57) is also calculated numerically. We have checked the two definitions of $\delta\Delta\beta$ and it turned out that the two definitions give the almost same result. This indicates the validity of our procedures.

2.4 Numerical Simulation

2.4.1 Update Program

Our update program consists of two algorithms, the pseudo-heat bath[37] and the over-relaxed[38] algorithm. The pseudo-heat bath algorithm is a standard method widely used for generation of SU(3) gauge configurations and it is more efficient than the Metropolis algorithm[39]. The over-relaxed algorithm is combined with the pseudo-heat bath algorithm so that decorrelation between configurations is accelerated. The decorrelation rate in terms of the autocorrelation time has been studied using blocked Wilson loops[14, 18, 19]. Due to the difficulty of measuring the autocorrelation time, however, a drastic improvement of decorrelation has not been seen yet. Even if so, there is a merit in using the over-relaxed algorithm. It is faster to update a lattice system than pure pseudo-heat bath algorithm[22]. Our update speed for the pseudo-heat bath algorithm is 2.6 μsec/link. On the other hand, one for the over-relaxed algorithm is 2.0 μsec/link. In updating, we use the pseudo-heat bath and the over-relaxed algorithm stochastically in a ratio of 1:9.

Our programs are developed on the parallel computer AP1000 in Fujitsu laboratory[21, 22]. This machine has 512 floating processors and can be extended to a 1024 processors version at maximum. The total speed of AP1000 with 512 processors is 4.3Gflops. The sustained speed for our program is about 60% of the total speed. Each processor has 16Mbytes memory. Hence AP1000 with 521 processors has 8Gbytes memory. The huge memory became a great advantage to develop flexibly a program for the blocking[22].

2.4.2 Configurations

We generate three sizes of a lattice, 32^4, 16^4 and 8^4, for our purpose. All the configurations are made at cold start, that is, all links are initially set to the unit matrix $U = I$. We update configurations typically up to 20,000-100,000th sweep.

Fist 2,000-10,000 sweeps are used for thermalization. The independence between configurations can be monitored by a measurement of the autocorrelation time. The blocked Wilson loops are also used for operators for the autocorrelation measurement since it contains a long range property of the lattice system[14]. It turned out that the blocked Wilson loop is useful to see a occurrence of a finite temperature phase transition of the system. This study has been done[18, 19, 20] and it has been showed that the autocorrelation time has a pronounced peak at finite cross over or finite temperature phase transition point. This means that at the finite cross over point it is very hard to obtain statistically independent configurations. Actually, we generated configurations of 30,000 sweeps on a 32^4 lattice at $\beta = 7.0$, where the system is considered to be at or near the deconfinement phase transition point. However no meaningful results could obtain due to the large autocorrelation. Then we decided not to use there configurations for the analysis.

2.5 Measurement of Wilson loop

As mentioned in Sec.2.3.2, $\Delta\beta$ can be determined by the matching method. At first a value of $\Delta\beta$ is determined for each Wilson loop and each q parameter. And then $\Delta\beta$ is extrapolated as a linear function of q. We have chosen three points, $q = \{0.0, 0.002, 0.004\}$. We measure 6 Wilson loops for purpose of the matching method. The shape of those Wilson loops are displayed in Fig.1 and we call them W11, W12, W22, Wchair, Wtwist and Wsofa respectively.

What we have to do in the matching method is evaluate β' which satisfies e.q.(2.47) by comparing values of Wilson loops. For this purpose, We have done Monte Carlo run at a number of β points. We have simulated at 96 points, from $\beta = 5.3$ to $\beta = 9.5$ on a 8^4 lattice and at 33 points, from $\beta = 5.75$ to $\beta = 7.7$ on a 16^4 lattice. Values of W11 operator for each level are plotted in Fig.8 as an example.

2.6 Results of $\Delta\beta$

2.6.1 Optimal value of q parameter

$\Delta\beta$ is determined for each Wilson loop operator, each q parameter and each blocking level. So we can write $\Delta\beta$ as:

$$\Delta\beta = \Delta\beta_l^{(i)}(q_m) \tag{2.58}$$

where i indicates the Wilson loop operator and l means the number of the blocking steps and we call it *Level*. As mentioned in Sec.2.3.2., we express $\Delta\beta_l^{(i)}(q_m)$ as a linear function of q and determine $\Delta\beta$ at an optimal q point where those lines intersect each other maximally.

Fig.9(a)-(d) shows how the optimal q's are determined or how values of $\Delta\beta$ are obtained. Those data are from matching of the 32^4 lattice at $\beta = 6.8$ and the 16^4 ones. It is seen that a functional dependence of $\Delta\beta$ is nicely expressed by a linear function of q. We can see some features of q dependence of $\Delta\beta$. At level 1, the q dependence of $\Delta\beta$ is strong, that is, the slope of the line is very steep. And we can see no good intersection for those lines. This indicates that the blocking scheme we took can not be optimized by only the q parameter such that the blocked trajectory can reach the renormalized trajectory after one blocking step. On the other hand, it is seen that the intersection is getting good as we go to high blocking level. It is noted that the data are presented in finer scale in Fig.9(d). So matching at Level 4 is not worse in comparison with those at Level 3. The q dependence of $\Delta\beta$ becomes weak as blocking goes on. This trend seems natural due to the following reason. As mentioned in Sec.2.3.2, this means that the blocking flow comes close to the renormalized trajectory after enough many blocking steps even if we start with a bad blocking scheme, that is, a blocking scheme with a non-optimal q parameter. Hence if we employ further blocking step at the level 4, we will see an approximate non-q-dependence of $\Delta\beta$.

We plot values of optimal q for each level in Fig.10. The values of q_{opt} at Level 2 and 3 are almost same. This indicates that after 2nd blocking step, the blocked

trajectory is already close to the renormalized trajectory. On the other hand, that of q_{opt} at Level 1 is very different, almost constant. This also means that we can not optimize the blocked trajectory tuning only the q parameter so that the blocked trajectory reaches to the renormalized trajectory by one blocking step. Even if the optimal value for Level 1 in Fig.10 is used, the blocked trajectory is still not close to the renormalized trajectory. Therefore values of $\Delta\beta$ at Level 1 can not be accurate.

2.6.2 $\Delta\beta$

In Fig.11 we plot $\Delta\beta$ obtained at each level on 32^4 lattices as a function of Level. For all β, we can see the same functional dependence, that is, $\Delta\beta$ decreases as Level increases and seems to converge to a constant value after Level 3, that is, 3rd blocking step. Although at Level 1 the value of $\Delta\beta$ is very different from others, at level 2 the value of $\Delta\beta$ is close to the stable value at Level 3 and 4. This behavior supports the interpretation for the approach to the renormalized trajectory as mentioned in Sec.2.6.1. Namely we can not optimize the blocking scheme by one blocking step. Therefore again we conclude that at Level 1 the value of $\Delta\beta$ is not accurate. At Level 2 the blocked trajectory is already close to the renormalized trajectory but not sufficient to obtain a reliable value. Therefore we can see a slight but clear difference between Level 2 and Level 3, 4.

Here note that situation on the approach to the renormalized trajectory is dependent on the blocking scheme we have taken. In this sense, good blocking scheme is the one which come close to the renormalized trajectory within first a few steps. Although we have taken the q parameter as an optimization parameter, there is another choice of an optimization parameter. For instance, it is possible to use the parameter a and b in e.q.(2.26) as an optimization parameter and there exists a work in which the parameter a and b are used as optimization parameters[12].

In Fig.12 we plot $\Delta\beta$ from 16^4 lattices for each level. As mentioned above,

$\Delta\beta$ at Level 1 are not accurate and very different from $\Delta\beta$ at Level 2 and 3. For level 2 and 3, $\Delta\beta$ are very similar each other but for $\beta \geq 6.4$, values of $\Delta\beta$ at Level 3 are systematically small. One of the possibilities of interpretation for this behavior is that $\Delta\beta$ is affected by the finite temperature phase transition since the transition point is about $\beta \approx 6.4$ on a 16^4 lattice and for $\beta \geq 6.4$ the system of a 16^4 lattice is in the deconfinement region. As already mentioned in Sec.1.1 one of the reasons we use a 32^4 lattice is we can remain in the confinement region till about $\beta \approx 7.0$ and we can avoid the systematic error coming from the phase transition. We plot $\Delta\beta$ at the deepest level from 16^4 and 32^4 lattice together in Fig.13. These values are summarized in Table 2.6.2.

Table 2.6.2(a) 16^4 lattice

β	$\Delta\beta$	*error*	β	$\Delta\beta$	*error*	β	$\Delta\beta$	*error*
5.85	0.323	0.007	6.25	0.430	0.009	6.60	0.545	0.045
5.90	0.317	0.013	6.28	0.422	0.011	6.65	0.507	0.013
5.95	0.325	0.010	6.30	0.432	0.010	6.70	0.527	0.030
5.98	0.334	0.004	6.35	0.448	0.012	6.75	0.500	0.010
6.00	0.338	0.007	6.38	0.457	0.012	6.80	0.535	0.027
6.03	0.343	0.007	6.40	0.454	0.013	6.85	0.511	0.025
6.05	0.351	0.005	6.43	0.460	0.011	6.90	0.531	0.028
6.10	0.366	0.006	6.45	0.485	0.006	7.00	0.539	0.017
6.12	0.372	0.013	6.47	0.468	0.011	7.20	0.546	0.041
6.15	0.390	0.003	6.50	0.461	0.005	7.35	0.568	0.048
6.17	0.387	0.015	6.53	0.478	0.016	7.50	0.557	0.019
6.20	0.387	0.007	6.55	0.521	0.020	7.60	0.579	0.078
6.23	0.418	0.009						

Table 2.6.2(b) 32^4 lattice

β	$\Delta\beta$	*error*
6.35	0.433	0.004
6.55	0.481	0.014
6.65	0.500	0.015
6.80	0.536	0.010

All the $\Delta\beta$ from 32^4 lattice are results in the confinement region. We can not see significant difference between $\Delta\beta$ from 16^4 and one from 32^4 lattices even if $\Delta\beta$ from 16^4 lattices are from the deconfinement region. However $\Delta\beta$ from the deconfinement region have large error and fluctuate very much. In Fig.13, we also line the prediction of $\Delta\beta$ from the 2 loop β function, e.q.(1.20), which is indicated as *bare* g^2. There is a clear discrepancy between $\Delta\beta$ from MCRG and one from the 2 loop prediction till about $\beta \simeq 7.5$ Although the discrepancy decreases as β increases, there is still a 10 % discrepancy at $\beta = 7.0$. From this, we may say that there is no asymptotic scaling below $\beta = 7.0$. This result is very serious for Monte Carlo simulation since the current simulation has been typically carried out at about $\beta = 6.5$ on the largest lattice such as 32^4 lattice and at $\beta = 6.5$ there is a 20 % discrepancy. As we will see in the next section, the asymptotic scaling violation can be reduced by some remedies.

2.7 Improved couplings

As we have seen above, the large deviation from the prediction with the 2-loop β-function still remains above $\beta \simeq 7.0$. However this situation can be improved by changing the scheme of the coupling to a mean field scheme[40] or an effective coupling scheme[41, 42] in stead of using 'poor' bare coupling.

Lepage and Mackenzie[40] have showed that the choice of the lattice bar coupling g^2 is not practical. For instance, let us take a look at the plaquette. In the

perturbative expansion, the plaquette value is expressed by[44, 43]:

$$< U_{plaq} >_{pt} = 1 - c_1 g^2 - c_2 g^4 - c_3 g^6 + ... \tag{2.59}$$

where the coefficients c_1, c_2 and c_3 are

$$c_1 = \frac{N^2 - 1}{8N} \tag{2.60}$$

$$c_2 = (N^2 - 1)(0.0204277 - \frac{1}{32N^2})\frac{1}{4} \tag{2.61}$$

$$c_3 = (N^2 - 1)N\left(0.0066599 - \frac{0.020411}{N^2} + \frac{0.0343399}{N^4}\right)\frac{1}{6} \tag{2.62}$$

where N is the number of colors. At $\beta = 6.0$, e.q.(2.59) with only the first two terms gives us:

$$< U_{plaq} >_{pt} \simeq 0.667. \tag{2.63}$$

On the other hand, from the Monte Carlo simulation, we obtain:

$$< U_{plaq} >_{MC} \simeq 0.597. \tag{2.64}$$

There is still 11% discrepancy between the perturbative calculation and the Monte Carlo calculation although the coupling in terms of $\alpha = g^2/4\pi$ is already small ($\alpha \simeq 0.08$). Therefore we may conclude that the bare lattice coupling g^2 fails to reproduce values of the plaquette correctly. In Ref.[40], the more continuum like coupling scheme or the mean field scheme has been proposed:

$$\frac{1}{g^2_{\overline{MS}}}(\pi/a) = \frac{< U_{plaq} >}{g^2(\pi/a)} + 0.008204N \tag{2.65}$$

where the new coupling is denoted as $g^2_{\overline{MS}}$ since this coupling exactly corresponds to the modified minimal subtraction ($\overline{MS}$) scheme in the continuum limit ($a \longrightarrow 0$). The relation between $g^2_{\overline{MS}}$ and g^2 coupling is known by the perturbative calculation[45]:

$$\frac{1}{g^2_{\overline{MS}}}(\pi/a) = \frac{1}{g^2(\pi/a)} - \frac{N^2 - 1}{8N} + 0.008204N. \tag{2.66}$$

Using e.q.(2.59) it is easily verified that e.q.(2.65) goes to e.q.(2.66) in the continuum limit. Therefore the scale parameter of the scheme defined by e.q.(2.65) takes the same value of $\Lambda_{\overline{MS}}$. Assuming the 2 loop β-function (e.q.(1.13)) for this coupling, and following the definition of Ref.[46] we obtain $\Lambda_{\overline{MS}}$ as:

$$a(x)\Lambda_{\overline{MS}} \equiv f_2^{\overline{MS}}(x) = \pi \left(\frac{x + b_1/b_0}{b_0} \right)^{b_1/2b_0^2} \exp\left(-\frac{x}{2b_0} \right) \tag{2.67}$$

where $x = \frac{1}{g^2_{\overline{MS}}}$ for the later convenience. Note that this definition is a little different from the definition of e.q.(1.16). Here we write it again for the later convenience:

$$a(x)\Lambda_L \equiv f_2(x) = \left(\frac{x}{b_0} \right)^{b_1/2b_0^2} \exp\left(-\frac{x}{2b_0} \right). \tag{2.68}$$

Using e.q.(2.67) and e.q.(2.68) the relation between $\Lambda_{\overline{MS}}$ and Λ_L in the continuum limit is easily obtained:

$$\frac{\Lambda_{\overline{MS}}}{\Lambda_L} = \lim_{a \to 0} \frac{f_2^{\overline{MS}}(1/g^2_{\overline{MS}})}{f_2(1/g^2)} = \pi exp(-\Delta/2b_0) \simeq 28.81 \tag{2.69}$$

where

$$\Delta = -\frac{N^2 - 1}{8N} + 0.008204N. \tag{2.70}$$

The ratio of $\Lambda_{\overline{MS}}$ and Λ_L is very large.

The other improved coupling, the effective coupling, is proposed by Karsch and Petronzio[42] motivated by Parisi[41]. They have proposed the g_e^2 coupling as follows:

$$g_e^2 = \frac{1 - < U_{plaq} >}{c_1} \tag{2.71}$$

where c_1 is the value of (2.60). Using the perturbative expansion of e.q.(2.59), we obtain:

$$g_e^2 = g^2 + \frac{c_2}{c_1} g^4 + \frac{c_3}{c_1} g^6 + O(g^8) \tag{2.72}$$

or

$$\frac{1}{g_e^2} = \frac{1}{g^2} - \frac{c_2}{c_1} + O(g^2). \tag{2.73}$$

Assuming the 2 loop β-function for this coupling and using e.q.(2.68) as a definition of the scale parameter Λ_e for this coupling:

$$a\Lambda_e = f_2(x) \tag{2.74}$$

where $x = \frac{1}{g_e^2}$, the relation between Λ_e and Λ_L is obtained by:

$$\frac{\Lambda_e}{\Lambda_L} = \lim_{a\to 0} \frac{f_2(1/g_2^2)}{f_2(1/g^2)} = \exp\left(\frac{c_2}{2c_1 b_0}\right) \simeq 2.0756 \tag{2.75}$$

and we also obtain the ratio of $\Lambda_{\overline{MS}}$ and Λ_e:

$$\frac{\Lambda_{\overline{MS}}}{\Lambda_e} = \frac{\Lambda_{\overline{MS}}}{2.0756\Lambda_L} = 13.88 \tag{2.76}$$

Bali and Schilling[43] have used the similar coupling, g_{e2}^2, defined by:

$$c_1 g_{e2}^2 + c_2 g_{e2}^4 = 1 - < U_{plaq} > \tag{2.77}$$

where c_1 and c_2 are taken from (2.60) and (2.61). Using the perturbative expansion e.q.(2.59), we obtain the inverse of g_{e2}^2:

$$\frac{1}{g_{e2}^2} = \frac{1}{g^2} + O(g^2). \tag{2.78}$$

Therefore the scale parameter for the coupling g_{e2}^2 is unchanged:

$$\Lambda_{e2} = \Lambda_L. \tag{2.79}$$

The qualitative behavior of the coupling g_{e2}^2 is similar with that of the coupling g_e^2[43].

Using these improved couplings, we compare $\Delta\beta$ from the MCRG study with one from the 2 loop β-function with the improved couplings. The curve M in Fig.14 shows the coupling shift $\Delta\beta$ from the $g_{\overline{MS}}^2$ coupling. This scheme partially explains our results of $\Delta\beta$. However the large deviation is still seen at low β($\beta \leq 6.6$). Similar analysis is also implemented for the effective coupling scheme, g_e^2. The curve E in Fig.14 is $\Delta\beta$ from the effective coupling scheme. This scheme also partially accounts for our results of $\Delta\beta$.

Now we consider the possibility to obtain further improvements. Let us introduce a next order correction in the β-function and define a new effective coupling g_u^2:

$$-\frac{dx_u}{2d\ln a} = b_0 + \frac{b_1}{x_u} + \frac{b'}{x_u^2} \tag{2.80}$$

where

$$x_u = \frac{1}{g_u^2} = \frac{1}{g_{\overline{MS}}^2} - x_0. \tag{2.81}$$

Here b' and x_0 are not known and these values are determined so that this coupling scheme accounts for $\Delta\beta$ form the MCRG study. Assuming the correction term b' is small, the integration of e.q.(2.80) leads to (See Appendix B):

$$a(x_u)\Lambda_u \equiv f(x_u) = f_2(x_u)\exp(\frac{-b'}{2b_0^2 x_u}). \tag{2.82}$$

where the function $f_2(x_u)$ comes from e.q.(2.68).

Using x_0 and b' as free parameters, we attempted two fits for the data of $\Delta\beta$ above $\beta = 6.0$:

(A) introduces only b'.

(B) introduces both x_0 and b'.

The case of (A) allows to add the correction term $O(g_u^7)$. The results are shown in Fig.14 as curve A. Unfortunately this case gives only a poor fit and the coefficient b' is relatively large against b_0: $b'/b_0 = -0.085(0.0013)$ (Note that $b_1/b_0 = 0.0587$).

The case of (B) allows x_0 and b' as free parameters. This case has a quit well fit for all the data of $\Delta\beta$(curve B in Fig.14). The values of parameters obtained by the fit are:

$$x_0 = 0.442(0.004) \tag{2.83}$$

$$b'/b_0 = -0.0119(0.0008) \tag{2.84}$$

The coefficient b' is small however the shift x_0 is non-negligible. In this scheme with the shift x_0, the relation to the $(\overline{MS})$ scheme in the continuum limit is obtained by:

$$\Lambda_u = \exp\left(\frac{x_0}{2b_0}\right)\Lambda_{\overline{MS}} = 23.95\Lambda_{\overline{MS}} \tag{2.85}$$

Therefore, Λ_u is $O(GeV)$ and much larger than $\Lambda_{\overline{MS}}$. Although we have better scaling in this scheme,this fact needs a explanation. At present, however , we have no reasonable explanation yet.

2.8 Scaling Test

Based on various improved couplings introduced above, we exam the scaling of the physical quantities in the unit of $\Lambda^{(0)}_{\overline{MS}}$ where (0) means we are employing the quenched case, $n_f = 0$. First we exam the string tension, one of popular physical observables in the Monte Carlo simulation. The data of string tensions come from Ref.[43]. Using various couplings, we plot the ratio of the string tension and the $\Lambda^{(0)}_{\overline{MS}}$ parameter in Fig.15. As shown in e.q.(1.18), those values should be constant in the asymptotic scaling region. The rightest value corresponds to one from $\beta = 5.7$ and the leftest value is from $\beta = 6.8$. We can see the large asymptotic scaling violation for the lattice bare coupling g^2. The improved couplings $g^2_{\overline{MS}}$ and g^2_e can reduce the asymptotic scaling violation as we see in Fig.15. However the visible deviation still remains. This situation needs the further interpolation to the continuum limit in order to obtain the continuum physics. On the other hand, the g^2_u coupling based on our MCRG results gives us a good improved scaling behavior. The values of $\sqrt{\sigma}/\Lambda^{(0)}_{\overline{MS}}$ are a nearly constant in the whole region $(5.7 < \beta < 6.8)$. The estimated value is:

$$\frac{\sqrt{\sigma}}{\Lambda^{(0)}_{\overline{MS}}} = 2.2(1). \tag{2.86}$$

Assuming $\sqrt{\sigma} = 440MeV$ as a input value, we can obtain the value of $\Lambda^{(0)}_{\overline{MS}}$:

$$\Lambda^{(0)}_{\overline{MS}} = 200MeV. \tag{2.87}$$

This value is smaller than that obtained by the extrapolation to the continuum limit using the coupling g^2_e in Ref.[43] where $\Lambda^{(0)}_{\overline{MS}} = 233MeV$.

Further test for other quantities are attempted. Fig.16 shows the test for the charmonium 1p-1s splitting[47]. We can see the similar scaling behavior. The

values from the coupling g_e^2 are almost constant and we obtain:

$$\frac{M_c}{\Lambda_{\overline{MS}}^{(0)}} = 2.1 \tag{2.88}$$

Substituting $M_c = 450MeV$ into e.q.(2.88), we obtain:

$$\Lambda_{\overline{MS}}^{(0)} = 210MeV. \tag{2.89}$$

Fig.17 shows the test for glueball 0^{++} mass. In this case, it seems that the ratio of glueball mass and $\Lambda_{\overline{MS}}^{(0)}$ from the improved couplings increases as β increases even if g_u^2 coupling is used. Hence for glueball 0^{++} mass, a good scaling behavior is not seen.

From above scaling tests, we can learn the followings:

(1) The improvements of the improved couplings (including g_u^2) are only partial since in the asymptotic scaling region, all the physical quantities should show the asymptotic scaling behavior.

(2) It is difficult to obtain reliable values in the continuum limit. Careful extrapolations to the continuum limit should be needed at this stage.

Chapter 3

Perfect Action Search

3.1 Effective Action on the blocked trajectory

As we have seen in Chapter 2, the standard Wilson action has a poor scaling property and even if we use the improved couplings the complete asymptotic scaling is not seen. As mentioned in Chapter 1, there is a possibility to use an improved action, such as *perfect action*. The perfect action, which defined on the renormalized trajectory, contains only a relevant interaction with respect to scale transformation. Therefore it is expected that the perfect action has a almost complete scaling behavior.

Our motivation to find an effective action for blocked gauge configuration is as follows. If we can offer an effective action or renormalized couplings on the blocked trajectory after enough blocking steps, we can obtain a perfect action since the blocked trajectory flows along the renormalized trajectory lastly .

There exists, however, a difficulty that it is very hard to directly determine the effective action or renormalized couplings since the effective action can be complicated enough with many couplings. And if we truncate some couplings it is also hard to know the effect of the truncation.

There are several ways to find an effective action for a given set of gauge configurations. Swendsen[48] has proposed a minimization procedure to find renor-

malized couplings, however, this method requires a good starting point and it becomes more difficult to give the good starting point as we deal with a complicated action. Creutz[49] has invented the microcanonical demon method and it has been applied to determine renormalized couplings on an SU(2) configuration with fundamental and adjoint couplings[50]. In actual applications, however, the method works poorly and the couplings obtained by the method have large systematic errors due to finite size effect. These errors are caused by extra degrees of freedom of the demons which carry a considerable part of the energy in a small system. Recently an idea, the canonical demon method, which does not cause systematic errors has been advocated and applied for $O(3)$ non-linear σ-model[51]. Although the idea is rather simple, the results coming from it are highly reliable. In this chapter we implement this method for a physically interesting case, SU(3) gauge theory and obtain the effective action on blocked configurations[52].

3.2 The Demon Method

Let us consider a configuration which is produced with a probability distribution:

$$P(U) \propto \exp(-\beta S[U]). \tag{3.1}$$

Now we introduce a demon into the lattice and consider a joint system of the lattice and the demon. On the joint system, the microcanonical partition function is written as:

$$Z_{Mic} = \sum_{E_d} \sum_{U} \delta(S[U] + E_d - E_{initial}) \tag{3.2}$$

where $E_{initial}$ is a total energy of the joint system which is initially determined and kept constant, and E_d is the demon energy. Notice that we need not a priori know information of the coupling to do the microcanonical step. After enough microcanonical sweeps, the demon energy is distributed with the Boltzmann's distribution:

$$P(E_d) \propto \exp(-\beta E_d). \tag{3.3}$$

In the thermodynamic limit, the average of the demon energy is given by:

$$< E_d >= \int E_d \exp(-\beta E_d) dE_d / Z \tag{3.4}$$

where Z is a partition function given by integrating out e.q.(3.3) with respect to the demon energy. The range of integration is taken suitably . We restrict the energy to $-E_{max} < E_d < E_{max}$. In this case, e.q.(3.4) becomes(See AppendixC):

$$< E_d >= \frac{1}{\beta} - E_{max} / \tanh(\beta E_{max}). \tag{3.5}$$

This equation gives a relation between $< E_d >$ and β. The coupling β can be obtained through the average demon energy by solving the above equation.

The extension to many couplings is straightforward. In this case, for each coupling we must introduce a corresponding demon. Therefore the corresponding microcanonical partition function is given by:

$$Z_{Mic} = \sum_{E_d^i} \sum_{U} \prod_{i} \delta(S^i[U] + E_d^i - E_{initial}^i), \tag{3.6}$$

and the coupling β^i corresponding to E_d^i is obtained by:

$$< E_d^i >= \frac{1}{\beta^i} - E_{max} / \tanh(\beta^i E_{max}). \tag{3.7}$$

In the microcanonical step, the demon visits one of links on a lattice and tries to change the link, that is, a new SU(3) matrix is taken from SU(3) group and the link is replaced with it. This trial change causes a shift of energy on the lattice, ΔE, which must be compensated with the demon energy since the total energy on the system is kept constant during the microcanonical update. After this trial change, new demon energy is given by:

$$E_d^{new} = E_d^{old} - \Delta E. \tag{3.8}$$

If the new demon energy remains in the allowed region, in the above case $-E_{max} < E_d^{new} < E_{max}$, this trial change is accepted. If not the case, the demon moves to

a next link keeping its old energy. In order to raise an acceptance ratio of the microcanonical update, it is possible to do some trial changes before the demon moves to a next link. If a number of demons are introduced in the system, the trial change is accepted only when all the demons remain in the allowed region. After adequate microcanonical sweeps, the demon moves into another configuration keeping its energy to make itself canonical[51].

3.3 Testing the demon method

In order to examine effectiveness of the method, first, we test the method for SU(3) gauge configurations generated on a 4^4 lattice with an action with 7 couplings(For those values see Table 3.1.) corresponding to the Wilson loop operators in Fig.1. We choose rather small lattice, 4^4 lattice, to test how the method works since it is getting worse to obtain the effective action as the lattice size becomes small. The action S is written as:

$$S = \sum_{i=1}^{7} \beta_i \sum_{W_i} ReTr(W_i)/3 \tag{3.9}$$

where W_i is a Wilson loop corresponding to one in Fig.1. Our numerical description is as follows.

Table 3.1: Coupling values used for update of a 4^4 lattice(the first row "**A**") and coupling values obtained by the demon method(the second row "**B**").

	β_{11}	β_{12}	β_{22}	β_{chair}	β_{sofa}	β_{twist}	$\beta_{4Dtwist}$
A	5.5	1.0	−0.1	−0.1	−0.1	−0.1	−0.1
B	5.5029(84)	1.0004(32)	−0.1027(37)	−0.0988(18)	−0.10032(94)	−0.0988(34)	−0.1028(12)

We need to introduce 7 demons, one for each of the 7 Wilson loop operators. Let us call the 7 demons "one demon system". We prepare 100 independent demon systems and 100 configurations and each demon system visits one of these configurations and the microcanonical update is carried out. Initially,

we set all the demons energy to zero. All the demons energy are restricted to $-10 < E_d < 10$ during the microcanonical step. After 100 microcanonical sweeps, each demon system, keeping its demon energy, moves into a second configuration taken from a next set of 100 configurations such that this second configuration is statistically independent to the first one. This procedure eliminates the systematic error due to the finite volume of the system. After another 100 microcanonical sweeps on the second configuration, each demon system again moves into a third configuration, and so on.

Fig.18 shows the demon energy averaged over the 100 demon systems for every sweep. On each configuration used by a demon system, after some microcanonical sweeps, the demon energy seems to be thermalized. However a clear difference of the demon energy between the first configuration and the second one can be seen. Although there also remains a difference between the second one and the third one, the difference is much smaller and seems to go to zero within thermal fluctuation. This behavior can be seen more clearly in Fig.19.

Fig.19 shows the average of the demon energy which correspond to the 5 couplings: $\beta_{22}, \beta_{chair}, \beta_{sofa}, \beta_{twist}$ and $\beta_{4Dtwist}$, on the first, second, etc configuration used by a demon system. We averaged over the last 20 microcanonical sweeps(We are doing 100 microcanonical sweeps on one configuration.) and furthermore over the 100 demon systems. Note that the configurations are generated with the same value(-0.1) for these couplings, hence the average values should be same for these demons. On the first 3 configurations, however, a clear difference is seen, which might be considered due to the finite volume effect of the microcanonical update. After enough movements of the demon system, in this case 3 movements, the average value seems to converge to one value.

This elimination of the finite volume effect works in the following way. In the infinite volume limit, initial values of the demons energy are not so important since the demons carry only a vanishingly small percent of the energy of a system. On the other hand, in our case the system is so small that the initial values of

the demons energy become important. Since we have set all the demons energy to zero, on the first configuration the demons energy becomes distributed with a Boltzmann's distribution $\exp(-\beta' E_d^i)$ which is away from the true Boltzmann's distribution $\exp(-\beta E_d^i)$ due to the finite volume effect. The demons move into a second configuration keeping their energy with the wrong Boltzmann's distribution which have ever has a larger overlap with the true one than the initial distribution($E_d^i = 0$). On the second configuration, the demon energy becomes distributed with a Boltzmann's distribution which is ever closer to the true one. By doing further movements, the distribution of the demon energy converges to the true one. To check this scenario, we set initial values of the demons energy to values distributed with the true Boltzmann's distributions and did the microcanonical update. In this case, we obtained the desired demons energy on the first configuration.

The coupling values, which correspond to the demons energy in Fig.19, converted through e.q.(3.4) are shown in Fig.20. Each coupling nicely converges to the value of -0.1. We proceeded the method to the 22nd configuration and obtained coupling value corresponding to each demon averaging over the configurations except the first 3 configurations as thermalization. The couplings are well reproduced within a few percent error bar.(See Table 3.1.)

So far, we have restricted the demon energy to $-10 < E_d < 10$, however, there is no reason to do so. If the constraint is set to a wide region, the demon carries a large part of energy of the system. This enhances a systematic error. To see this, setting all the demons to $-50 < E_d < 50$, we performed the microcanonical update as above. Fig.21 shows the coupling value converted from average energy of the demon corresponding to β_{11} in the both regions, that is, $-10 < E_d < 10$ and $-50 < E_d < 50$. Although for the both cases, each demon energy seems to converge, the convergence of the demon energy in the wide region is very poor. From this point of view, it might be better to restrict the demons in a narrow region as possible as we can. As a matter of fact we can not take a very narrow

region, since the acceptance ratio of the microcanonical update goes to zero. Therefore the constraint to the demons energy should be optimized suitably.

3.4 The Demon Method on Blocked Configurations

As we have seen in the previous section, the demon method works very well. In this section, we implement the demon method for blocked SU(3) gauge configurations. Now the effective action is not known. The blocked configurations whose size is 4^4 are produced after twice blockings from 16^4 lattices with the Wilson action at $\beta = 6.2$ by QCD_TARO Collaboration[53]. The blocking scheme we take here is a double smeared blocking of a scale factor 2. With certain optimal parameters[30, 53] it does not induce complicated extended interactions corresponding to large Wilson loops in the classical level. The double smeared blocking is as follows.

A link $U_\mu(n)$ is smeared twice:

$$V_\mu(n) = (1-6c)U_\mu(n) + c\sum_{\nu\neq\mu} U_\nu(n)U_\mu(n+\nu)U_\nu{}^\dagger(n+\mu) \tag{3.10}$$

$$T_\mu(n) = (1-6c)V_\mu(n) + c\sum_{\nu\neq\mu} V_\nu(n)V_\mu(n+\nu)V_\nu{}^\dagger(n+\mu) \tag{3.11}$$

where $T_\mu(n)$ and $V_\mu(n)$ are once and twice smeared link respectively. The two adjacent smeared links are connected as:

$$Q_\mu(n) = T_\mu(n)T_\mu(n+\mu) \tag{3.12}$$

and a blocked link $U_\mu^{(b)}(n)$ is obtained according to a probability distribution:

$$P(U_\mu^{(b)}(n)) \propto \exp\left(\kappa\beta ReTr(U_\mu^{(b)}(n)Q_\mu^\dagger(n))/3\right) \tag{3.13}$$

The parameters, c and κ, are tuned so that the effective action becomes local. Here we take $c = 0.077$ and $\kappa = 10.5$[30, 53].

Assuming that the effective action has only 7 nterctions as in Fig.2, we do the same procedure as above. Fig.22 shows the coupling value of β_{11} converted through the demon energy at each configuration. In this case, the demon energy seems to be already thermalized on the second configuration. The coupling values obtained by the demon method are summarized in Table 3.2. We can observe a coupling decay for those couplings, namely, the values of 8 links Wilson loop couplings is smaller than the values of 6 links ones. It might be conjectured that contributions from more than 8 links Wilson loops are smaller.

Table 3.2: Coupling values obtained by the demon method for the double smeared blocking(**D**) and Swendsen's blocking(**S**). The double smeared blocking is done at $\beta = 6.2$ and Swendsen's blocking is at $\beta = 6.0$.

	β_{11}	β_{12}	β_{22}	β_{chair}	β_{sofa}	β_{twist}	$\beta_{4Dtwist}$
D	1.1402(25)	0.1169(16)	0.0204(22)	0.20023(94)	0.03494(80)	0.1935(13)	0.07032(89)
S	6.236(45)	−0.7033(59)	0.0653(74)	−0.1042(34)	0.0300(30)	0.2151(66)	0.1023(13)

To verify the validity of the effective action obtained in this way we compare the values of a number of Wilson loop operators. The second row of Table 3.3 shows the values of these Wilson loop operators on the blocked configurations. The third row shows the ones measured on generated configurations with the effective action with the couplings of Table 3.2. They agree well within error bars. However this is not a severe check of the truncation effect since we measured only Wilson loops which the demons couple to. Unfortunately we did not measured such Wilson loops which the demons do not couple to.

Table 3.3: Values of the Wilson loop operators on the double smeared blocked configurations(**BL**) and on the configurations generated with the couplings obtained by the demon method(**GE**).

	W_{11}	W_{12}	W_{22}	W_{chair}	W_{sofa}	W_{twist}
BL	0.10119(34)	0.01814(21)	0.00177(11)	0.02585(16)	0.003253(59)	0.02137(15)
GE	0.10121(15)	0.018167(57)	0.001722(64)	0.025789(53)	0.003251(37)	0.021528(43)

We also measure susceptibilities between Wilson loop operators as another check. We define the susceptibilities σ_{ij}^2 as:

$$\sigma_{ij}^2 = < W_i W_j > - < W_i >< W_j >, \tag{3.14}$$

where $< ... >$ indicates taking an average. The susceptibilities obtained by this definition are summarized in Table 3.4. All the non-diagonal susceptibilities are correctly reproduced in sign. As for magnitude of the susceptibilities, most of them are correctly reproduced within 2 sigma error bar. There are small but definite deviations for those of W11-W11, Wchair-Wsofa, W12-Wtwist, and Wsofa-Wtwist. Therefore the obtained action is still an approximate one. Complete reproduction will be obtained by enlarging coupling constant space. However, such fine tuning is too premature for the first trial and we do not come into further detailed reproduction.

Table 3.4: Susceptibility σ_{ij} ($\times 1000$). In each row, upper figures from the double smeared blocked configurations and lower figures are from the configurations generated with the coupling by the demon method.

$W_i \downarrow, W_j \rightarrow$	W_{11}	W_{12}	W_{22}	W_{chair}	W_{sofa}	W_{twist}
W_{11}	7.55(13)	3.67(14)	1.57(27)	3.955(85)	1.55(11)	3.15(14)
	8.212(69)	3.833(57)	1.20(24)	4.084(39)	1.156(95)	3.172(52)
W_{12}		4.73(10)	1.36(23)	2.17(11)	1.257(68)	1.936(95)
		4.727(25)	1.37(11)	2.088(29)	1.007(82)	1.601(44)
W_{22}			5.98(11)	0.99(21)	0.78(20)	1.01(21)
			6.046(38)	0.59(16)	0.609(98)	0.74(17)
W_{chair}				3.183(40)	1.193(48)	2.522(55)
				3.130(19)	0.879(45)	2.387(29)
W_{sofa}					2.259(28)	1.412(82)
					2.192(19)	1.020(28)
W_{twist}						4.125(68)
						4.136(36)

We also implement the demon method for blocked configurations generated by

a different blocking, Swendsen's scale factor 2 blocking[32, 14, 18]. The blocking procedure we take is same as in Sec.2.1

Blocked configurations are also produced by QCD_TARO Collaboration[14, 22], after twice blockings with $q = 0$ from $32^3 \times 64$ lattices with the Wilson action at $\beta = 6.0$. These configurations have a size of $8^3 \times 16$. Therefore it can be expected that the finite volume effect is much smaller comparing to the case of a 4^4 lattice. As seen in Fig.10, the optimal q is about 0 at $\beta = 6.0$. Therefore we have blocked configurations with $q = 0$. In general, however, this optimal value does not necessarily mean that the effective action is local.

We introduced only one demon system and used 4 configurations, so far. Although in this case statistics might not be enough to obtain a definite result, at least we could obtain a interesting preliminary result and further investigation should be needed to improve statistics and verify the result. The result is given in Table 3.2 together with the double smeared blocking case. The interesting behavior is that although for the double smeared blocking all the couplings take positive values while for Swendsen's blocking some couplings take negative values and the β_{11} coupling is rather increasing. This is an example that the renormalized trajectory is dependent on what blocking scheme we take. Although for Swendsen's blocking we can also observe a coupling decay for those couplings, it is rather slow, namely, the β_{chair} coupling of a 6 links loop and the $\beta_{4Dtwist}$ coupling of a 8 links loop are nearly equal. So it might be probable that some truncation effects are still contained in the effective action which we obtained and they may be large. A careful analysis should be needed in further investigation in order to see the truncation effect.

Chapter 4

Conclusion

In Chapter 2 we have analyzed scaling property of the standard Wilson action in terms of the coupling shift $\Delta\beta$ using the MCRG technique. There was discrepancy in the previous results of $\Delta\beta$ and they were very controversial.

This is partly due to smallness of lattice size which limits blocking step and causes unwanted finite temperature phase transition at high β. Another point is lack of insufficient statistics.

To solve this, we have worked on 32^4 lattices and done high statistics Monte Carlo simulations. Our results have showed that there is a large deviation from the prediction of the 2 loop β-function up to $\beta \simeq 7.5$. From this analysis, we conclude that the standard Wilson action has not the perturbative scaling property at presently accessible β. Therefore in order to obtain values in the continuum limit using the standard Wilson action, some careful extrapolations to the continuum limit should be needed or we have to go to higher β, provided that the performance of computers is powerful enough.

Using the improved couplings, $g^2_{\overline{MS}}$ and g^2_e, however, the deviation can be reduced but it is only a partial improvement. For $\beta \leq 6.5$ the large deviation still remains.

We have proposed a new coupling scheme g^2_u which is determined so that it accounts for our $\Delta\beta$ results. And we have tested the scaling for the string tension,

the charmonium 1p-1s splitting and the glueball mass using g_u^2 and also bare g^2, $g_{\overline{MS}}^2$ and g_e^2. From this scaling test, we have found that the improved coupling $g_{\overline{MS}}^2$ and g_e^2 recover the scaling property partially but not completely. On the other hand, We have better scaling for the string tension and the charmonium 1p-1s splitting by the use of g_u^2 coupling in a region $5.7 < \beta < 6.8$. Using the g_u^2 coupling, $\Lambda_{\overline{MS}}$ of the continuum QCD is estimated to be $200MeV$ from the string tension and $210MeV$ from the charmonium 1p=1s splitting. These values are smaller than that given by g_e^2, $\Lambda_{\overline{MS}} = 233MeV$.

A point to be clarified in that scale parameter in the g_u^2 coupling scheme, Λ_u, is fairly large, a few GeV. At present, we have no reasonable explanation for this point and it is left for future investigations.

For the glueball 0^{++} mass, we could not see a good scaling even if the coupling g_u^2 is used for them.

We are able to take another approach to the scaling problem. That is to find an action of lattice QCD which is sitting on the renormalized trajectory and is named perfect action. If the perfect action is known and it is a very local action, it will be a useful and reliable action in the Monte Carlo simulations. As the first step of the investigation, we study a possibility to find effective action for blocked gauge configurations.

In Chapter 3 we have developed a tool, the demon method, to find the perfect action. First the method was tested for the known gauge configurations generated with the 7 couplings. We have successfully reproduced the 7 couplings within a few percent error bar. Based on this study, the method was then used on the double smeared blocked SU(3) gauge configurations and an effective action was obtained. To check the validity of the effective action we have generated configurations by this action and measured values of some Wilson loop operators. Their values turn out to be the same as those measured directly on the blocked configurations within error bars. Susceptibilities were also measured as another check. They showed the same sign in non-diagonal parts and the same magnitude

except small deviations on a few susceptibilities. Therefore we conclude that the demon method works very well to determine effective actions in multi-dimensional coupling constant space. It is considered that the demon method is a strong tool to find the perfect action which gives physical prediction in continuum space-time with good precision.[29] In principle, enough blocking transformations get the system close to renormalized trajectory even if we start with Wilson action. If an effective action is determined there, it becomes the perfect action. From this point of view, searching for the perfect action utilizing the demon method is very promising and an investigation in this direction is going on [53].

Acknowledgements

The study in Chapter 2 was carried out as a project of QCD_TARO collaboration. The author would like to thank to all the member of QCD_TARO collaboration: K.Akemi, Ph de Forcrand, M.Fujisaki, T.Hashimoto, S.Hioki, O.Miyamura, A.Nakamura, M.Okuda, I.O.Stamatescu and Y.Tago.

The study in Chapter 3 was pursued in part while he was staying at Institut für Theoretische Physik, Universität Heidelberg. He also thanks to I.Bender, J.Holk, M.Plewnia, I.O.Stamatescu and W.Wetzel for their warm hospitality.

Finally he especially thanks to O.Miyamura and M.Yonezawa for their constant encouragement.

Appendix A

Blocking Scheme

Here we give the proof that our blocking scheme is given by e.q.(2.36). Let us consider a simple case, one variable, and assume e.q.(2.36). A new blocked link U_b is given according to the probability distribution:

$$dU_b P(U_b) = dU_b \int dU \exp[-S[U] + N(Q) + pReTr(U_b(Q^\dagger Q)^{-\frac{1}{2}} e^{i\alpha/3} Q^\dagger)]. \quad \text{(A.1)}$$

Since U_b is an SU(3) matrix, it can be parametrized as:

$$U_b = VU' \quad \text{(A.2)}$$

where

$$V = Q(Q^\dagger Q)^{\frac{-1}{2}} e^{-i\alpha/3} \quad \text{(A.3)}$$

$$U' = \exp(i \sum_{l=1}^{8} c_l \frac{\lambda_l}{2}) \quad \text{(A.4)}$$

and λ_l are SU(3) generators and c_l are parameters. Using the property of the invariant measure, we obtain:

$$dU_b = d(VU') = dU' \quad \text{(A.5)}$$

Therefore e.q.(A.1) is rewritten as:

$$dU' P(U') = dU' \int dU \exp[-S[U] + N(Q) + pReTr(U')]. \quad \text{(A.6)}$$

This means that U' is taken according to the probability distribution:

$$dU'P(U') \propto dU' \exp(pReTr(U')) \tag{A.7}$$

The $ReTr(U')$ is expanded as:

$$\begin{aligned} ReTr(U') &= ReTr(\exp(i\sum_{l=1}^{8} c_l \frac{\lambda_l}{2})) && \text{(A.8)} \\ &= ReTr(1 + i\sum_{l=1}^{8} c_l \frac{\lambda_l}{2} - \frac{1}{4 \times 2!}\sum_{l,m} c_l \lambda_l c_m \lambda_m + ...) && \text{(A.9)} \\ &= 3 - \frac{1}{4}\sum_{l} c_l^2 + ... && \text{(A.10)} \end{aligned}$$

Assuming c_l are small, e.q.(A.7) is given by:

$$dU'P(U') \propto dU' \exp(p(3 - \frac{1}{4}\sum_{l} c_l^2)) \tag{A.11}$$

If c_l are small, the integration measure dU' is given as:

$$dU' = \prod_{l} dc_l \exp(-\frac{1}{8}c_l^2). \tag{A.12}$$

Therefore we obtain:

$$dU'P(U') \propto exp(3p) \prod_{l} exp(-(\frac{p}{4} + \frac{1}{8})c_l^2)dc_l. \tag{A.13}$$

This means that the parameter c_l are obtained according to the probability distribution:

$$P(c_l) \propto exp(-(\frac{p}{4} + \frac{1}{8})c_l^2). \tag{A.14}$$

Replacing $(p/4 + 1/8)$ with $1/2q$, we finally obtain:

$$P(c_l) \propto exp(-\frac{c_l^2}{2q}). \tag{A.15}$$

Hence U' is a gaussian matrix and U_b given by e.q.(A.2) corresponds to the blocked matrix of e.q.(2.33).

$N(Q)$ is a normalization factor and in the Monte Carlo simulation we do not need to care about it. $N(Q)$ is calculated as follows:

$$\begin{aligned} & \int \exp(3(\frac{2}{q}-\frac{1}{2}))\prod_l dc_l \exp(-\frac{c_l^2}{2q}) \\ = \;& \exp(3(\frac{2}{q}-\frac{1}{2}))(\sqrt{2q\pi})^8 \qquad (A.16) \\ \equiv \;& exp(-N(Q)). \qquad (A.17) \end{aligned}$$

Hence we obtain:

$$N(Q) = -\ln[\exp(\frac{2}{q}-\frac{1}{2})(2q\pi)^4]. \qquad (A.18)$$

Appendix B

Correction factor to the 2 loop formula

We want to integrate the following:

$$\int 2d\ln a = \int \frac{dx}{b_1 + \frac{b_1}{x} + \frac{b'}{x^2}} \tag{B.1}$$

where $x = 1/g_u^2$.

The right hand side is expanded as:

$$\frac{dx}{b_0 + \frac{b_1}{x} + \frac{b'}{x^2}} = \frac{dx}{b_0}(1 - A + A^2 - A^3 + A^4 - A^5 + ...) \tag{B.2}$$

where

$$A = \frac{b_1}{b_0 x} + \frac{b'}{b_0 x^2}. \tag{B.3}$$

Arranging the terms in e.q.(B.2), we obtain:

$$\frac{dx}{b_0 + \frac{b_1}{x} + \frac{b'}{x^2}} = \frac{dx}{b_0}\{(1 - \frac{b_1}{b_0 x} + (\frac{b_1}{b_0 x})^2 - (\frac{b_1}{b_0 x})^3 + ...) \tag{B.4}$$

$$-\frac{b'}{b_0 x^2} + \frac{2b_1 b'}{b_0^2 x^3} + (\frac{b'^2}{b_0^2} - \frac{3b_1^2 b'}{b_0^3})\frac{1}{x^4} + ...\} \tag{B.5}$$

We can recognize that e.q.(B.4) is an expansion of the contribution of the 2 loop β-function. Therefore the correction factor to the 2 loop formula is given by

e.q.(B.5) and this is easily integrated. We obtain the following formula as the correction factor up to $O(1/x^5)$.

$$\begin{aligned} a\Lambda_u &= f_2(x)\exp[\frac{1}{b_0}\{-\frac{c_2}{2x}+\frac{c_1c_2}{2x^2}+\frac{1}{6}(c_2^2-3c_1^2c_2)\frac{1}{x^3} \\ &\quad +\frac{1}{8}(4c_1^3c_2-3c_1c_2^2)\frac{1}{x^4}+\frac{1}{10}(6c_1^2c_2^2-c_2^3-5c_1^4c_2)\frac{1}{x^5}\}] \end{aligned} \tag{B.6}$$

where

$$c_1 = \frac{b_1}{b_0} \tag{B.7}$$

$$c_2 = \frac{b'}{b_0} \tag{B.8}$$

and $f_2(x)$ is the 2 loop formula. If we assume that the coupling $g_u^2 = 1/x$ is small enough, the correction factor is approximately given by the first term, $\exp(-\frac{c_2}{2b_0x})$.

Appendix C

Relation between the coupling and the demon energy

The partition function of the demon is given by:

$$Z = \int_{E_{min}}^{E_{max}} \exp(-\beta E_d) dE_d \tag{C.1}$$

$$= [-\frac{1}{\beta} \exp(-\beta E_d)]_{E_{min}}^{E_{max}} \tag{C.2}$$

$$= -\frac{1}{\beta}[\exp(-\beta E_{max}) - \exp(-\beta E_{min})] \tag{C.3}$$

where the integration rage is $E_{min} < E_d < E_{max}$. The expectation value of the demon energy is given by:

$$< E_d > = \frac{1}{Z} \int_{E_{min}}^{E_{max}} E_d \exp(-\beta E_d) dE_d \tag{C.4}$$

$$= \frac{1}{Z} \int_{E_{min}}^{E_{max}} -\frac{E_d}{\beta} \exp(-\beta E_d)' dE_d \tag{C.5}$$

$$= \frac{1}{Z}[-\frac{E_d}{\beta} \exp(-\beta E_d)]_{E_{min}}^{E_{max}} + \frac{1}{Z} \int_{E_{min}}^{E_{max}} \frac{1}{\beta} \exp(-\beta E_d) dE_d \tag{C.6}$$

$$= \frac{1}{Z}[-\frac{E_d}{\beta} \exp(-\beta E_d) - \frac{1}{\beta^2} \exp(-\beta E_d)]_{E_{min}}^{E_{max}} \tag{C.7}$$

The value of the coupling can be obtained by e.q.(C.7). Here we show the relations for several cases.

(1)$E_{min} = 0,\ E_{max} = \infty$

$$< E_d >= \frac{1}{\beta} \tag{C.8}$$

(2)$E_{min} = -E,\ E_{max} = \infty$

$$< E_d >= -E + \frac{1}{\beta} \tag{C.9}$$

(3)$E_{min} = 0,\ E_{max} = E$

$$< E_d >= \frac{1}{\beta}\left(1 - \frac{\beta E}{\exp(\beta E) - 1}\right) \tag{C.10}$$

(4)$E_{min} = -E,\ E_{max} = E$

$$< E_d >= \frac{1}{\beta} - E/\tanh(\beta E) \tag{C.11}$$

Bibliography

[1] K.G.Wilson Phys. Rev. D10 (1974) 2445

[2] M.Creutz Phys. Rev D21 (1980) 2308

[3] See for example, Y.Iwasaki Nucl. Phys. B (Proc. Suppl.) 34 (1994) 78

[4] See for example, D.Weingarten Nucl. Phys. B (Proc. Suppl.) 34 (1994) 29
A.Ukawa, Nucl.Phys. B(proc. Suppl.) 30 3 (1993) 3

[5] See for example, A.Nakamura, Acta Phys. Pol. B16 (1985) 635

[6] H.D.Politzer, Phys. Rev. Lett. 20 (1973) 1346
D.Gross and F.Wilczek, Phys. Rev. Lett. 30 (1973) 1343; Phys. Rev. D8 (1976) 3633

[7] A.Hasenfratz,P.Hasenfratz,U.Heller and F.Karsch, Phys. Lett. 140B (1984) 76; Phys. Lett. 143B (1984) 193

[8] K.C.Bowler et al., Nucl. Phys. B257[FS14] (1985) 155,

[9] K.C.Bowler et al., Phys.Lett. 179B (1986) 375

[10] R.Gupta,G.W.Kilcup,A.Patel and S.R.Sharpe, Phys. Lett. 211B (1988) 132

[11] R.Gupta,G.Guralnik,A.Patel,T.Warnock and C.Zemach, Phys. Rev. Lett. 53 (1984) 1721; Phys. Lett. 161B (1985) 352,

[12] J.Hoek, Nucl. Phys. B339 (1990) 732

[13] D.Petcher, Nucl. PHys. B275 [FS17] (1986) 241

[14] QCD_TARO collaboration: K.Akemi, Ph.de Forcrand, M.Fujisaki, T.Hashimoto, H.C.Hege, S.Hioki, J.Makino, O.Miyamura, A.Nakamura, M.Okuda, I.O.Stamatescu, Y.Tago and T.Takaishi, Nucl. Phys. B (Proc. Suppl.) 26(1992) 420

[15] QCD_TARO collaboration: K.Akemi et al, Nucl. Phys. B (Proc. Suppl.) 30 (1993) 517

[16] QCD_TARO collaboration: K.Akemi et al, Phys. Rev. Lett. 71 (1993) 3063

[17] QCD_TARO collaboration: K.Akemi et al, Nucl. Phys. B (Proc. Suppl.) 34 (1994) 246

[18] QCD_TARO collaboration: K.Akemi et al., Nucl. Phys. B (Proc. Suppl.) 30 (1992) 253

[19] QCD_TARO collaboration: K.Akemi et al., Nucl. Phys. B (Proc. Suppl.) 34 (1992) 789

[20] QCD_TARO collaboration: K.Akemi et al., Phys. Lett. B328 (1994) 407

[21] QCD_TARO collaboration: K.Akemi et al., Nucl. Phys. B (Proc. Suppl.) 26 (1992) 644

[22] QCD_TARO collaboration: K.Akemi et al., Quantum Chromodynamic Simulations on a Nondedicated Parallel Computer, Pre.YAMAGATA-HEP-93-11,IPS(ETHZ) Res.Rep No.93-64.

[23] K.Symanzik, in Recent developments in gauge theories, ed. G.'t Hooft et al. (Plenum, New York, 1980); Nucl. Phys. B226 187 (1983) 205

[24] K.G.Wilson, in Recent developments in gauge theories, ed. G.'t Hooft et al. (Plenum, New York, 1980)

[25] Y.Iwasaki, preprint UTHEP-118

[26] B.Berg et al., Comm. Math. Phys. 97 (1985) 31

S.Belforte et al., Phys. Lett. B137 (1984) 207

Ph. de Forcrand and C.Roiesnel, Phys. Lett. B127 (1984) 213

[27] Y.Iwasaki and T.Yoshie, Phys. Lett. B143 (19984) 449

S.Itoh et al. Phys. Lett. B148 (1984) 153; Phys. Lett. B167 (1986) 443; Phys. Rev. D33 (1986) 1806; Nucl. Phys. B274 (1986) 33

[28] Y.Iwasaki and T.Yoshie, Phys. Lett. B130 (1983) 77

M.Fukugita et al. Phys. Lett. B130 (1983) 73

[29] P.Hasenfratz and Niedermayer, Nucl. Phys. B414 (1993) 785

[30] A.Hasenfratz et al, in Lattice'94 Nucl. Phys. B(Proc. Suppl.) to be published

[31] S.K.Ma, Phys. Rev. Lett. 37 (1976) 461

[32] R.H.Swendsen, Phys. Rev. Lett. 42 (1979) 859

[33] R.Swendsen, Phys. Rev. Lett. 47 (1981) 1775

[34] R.Cordery et al., Phys. Lett. B128 (1983) 425

[35] D.Callaway and R.Petronzio, Phys. Lett. B149 (1984) 175

[36] A.Patel, Ph.D thesis, California Institute of Technology, 1984 (unpublished)

[37] N.Cabibbo and E.Marinari, Phys. Lett. B119 (1982) 387

[38] S.L.Adler Phys. Rev. D23(1981) 2901

F.R.Brown and T.J.Woch, Phys. Rev. B58 (1987) 2394

[39] M.Metropolis et al., J. Chem. Phys. 21 (1953) 1087

[40] G.P.Lepage and P.B.Mackenzie, Phys. Rev. D48 (1993) 2250

[41] G.Parisi, Proc. XXth Conf. on High Energy Physics (Madison 1980) ,p423.

[42] F.Karsch and R.Petronzio, Phys.Lett. 139 (1984) 403

[43] G.S.Bali and K.Schilling, Phys.Rev. D47 (1993) 661

[44] A. Di Giacomo and G.C. Rossi, Phys. Lett. B100 (1981) 481

B. Alleś et al., Pisa Report No. IFUP-TH-32192, 1992 (unpublished)

[45] A. and P. Hasenfratz, Phys. Lett B93 (1980) 165; Nucl. Phys. B193 (1981) 210

[46] Particle Data Group, J.J.Hernandez et al., Phys. Lett. B239 (1990) 1

[47] A.X.El-Khadra,G.Hockney,A.S.Kronfeld and P.B.Mackenzie , Phys. Rev. Lett. 69 (1992) 729.

[48] R.H.Swendsen, Phys. Rev. Lett. 52 (1984) 1165

[49] M.Creutz, Phys. Rev. Lett. 50 (1983) 1411

[50] M.Creutz, A.Gocksch, M.Ogilvie and M.Okawa, Phys. Rev. Lett. 53 (1984) 875

S.R.Das and J.B. Kogut, Phys. Lett. B179, 130 (1986)

[51] M.Hasenbush, K.Pinn and C.Wieczerkowski, Phys. Lett. B338 (1994) 308

[52] Some results for SU(3) gauge theory by the demon method have been presented in Lattice'94 in Bielefeld(See T.Takaishi, in Lattice'94 Nucl. Phys. B(Proc. Suppl.) to be published) See also T.Takaishi, Mod. Phys. Lett. A to be published

[53] QCD_TARO Collaboration, in Lattice'94 Nucl. Phys. B(Proc. Suppl.) to be published

Figure Captions

Figure 1: $\Delta\beta$ vs β, from previous results. The line *bare g* is from the 2 loop prediction.

Figure 2: Shape of Wilson loop operators. These Wilson loops except for $W_{4dtwist}$ are used for the matching method(Chapter 2). In the demon method(Chapter 3), all the Wilson loops are considered.

Figure 3: Fixed point action and Renormalized trajectory.

Figure 4: Blocking in spin system.

Figure 5: Wilson's scale factor $b = 2$ blocking. 8 links are summed up in 4 dimension. Here, 4 of them are drawn in 3 dimension. A new blocked link is put between 2 block sites.

Figure 6: Swendsen's scale factor $b = 2$ blocking.

Figure 7: Blocked trajectory and Renormalized trajectory. 2 blocked trajectories match on the Renormalized trajectory.

Figure 8:1×1 loop(plaquette) at each blocking level with $q = 0$. "Level 0" means no blocking procedure. "Level 1", Level 2" and "Level 3" mean blocking level.

Figure 9(a)-(d): Matching on a 32^4 lattce at $\beta = 6.8$. These

figures shows the interpolation at each blocking level. It is seen that the dependence of q becomes weaker at high blocking level. (Note that scale of Y axis are different at each blocking level.)

Figure 10: q_{opt} vs β, on 16^4 lattices.

Figure 11: $\Delta\beta$ vs blocking level, on 32^4 lattices.

Figure 12(a)-(b): $\Delta\beta$ at each blocking level on the 16^4 lattice vs β. Filled triangle, squares and filled circles indicate level 1, level 2 and level 3 respectively. Fig.12(a) is zoomed to Fig.12(b).

Figure 13: $\Delta\beta$ vs β for all data from this study. The solid line indicated as *bare* g^2 is the prediction from the 2-loop β function.

Figure 14: $\Delta\beta$ and fitted curves from various coupling schemes. The curve M is the result of $\Delta\beta$ from $g^2_{\overline{MS}}$ and the curve E is ones from g^2_e. The curve A and B means fitted curves with b' only and one with both b' and x_0 respectively.

Figure 15: Scaling test for string tension.

Figure 16: Scaling test for charmonium 1p-1s splitting.

Figure 17: Scaling test for 0^{++} glueball mass.

Figure 18: (a) Demon energy associating with β_{11} coupling at each microcanonical sweep. First, the demon visits a 1st configuration and then moves into a 2nd configuration and so on. (b) Same for β_{chair} coupling.

Figure 19: Average demon energy for $\beta_{22}, \beta_{chair}, \beta_{sofa}, \beta_{twist}$ and $\beta_{4Dtwist}$ on each configuration(1st, 2nd,..., n-th configuration).

Figure 20: Coupling value converted from the demon energy

in Fig.19.

Figure 21: Coupling value of β_{11} from the demon method in both regions of $-10 < E_d < 10$ and $-50 < E_d < 50$.

Figure 22: Coupling value of β_{11} from the demon method on the double smeared blocked configuration.

Figure 1

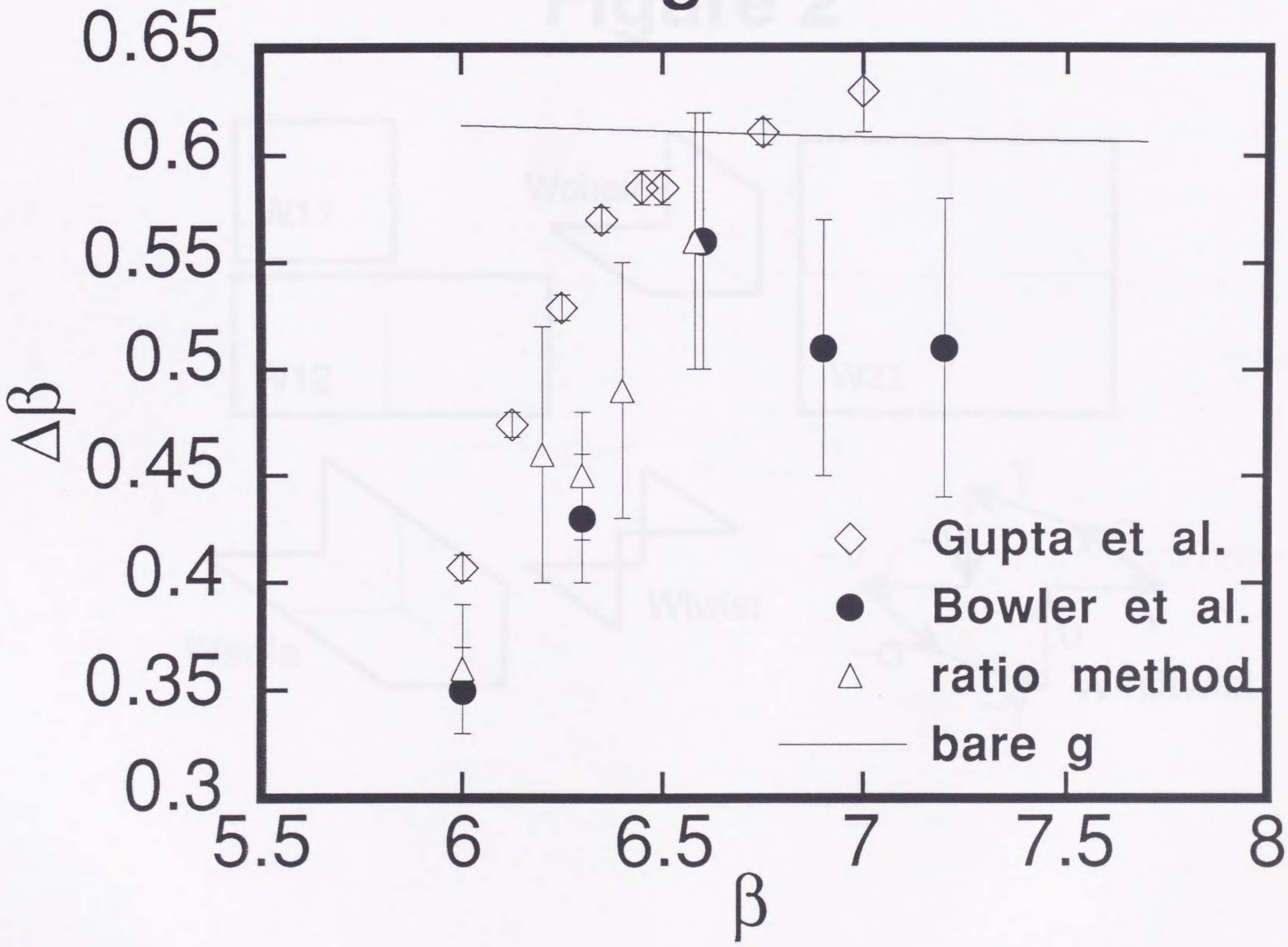
0.65
0.6
0.55
0.5
0.45
0.4
0.35
0.3
Δβ
5.5
6
6.5
7
7.5
8
β
Gupta et al.
Bowler et al.
ratio method
bare g

Figure 2

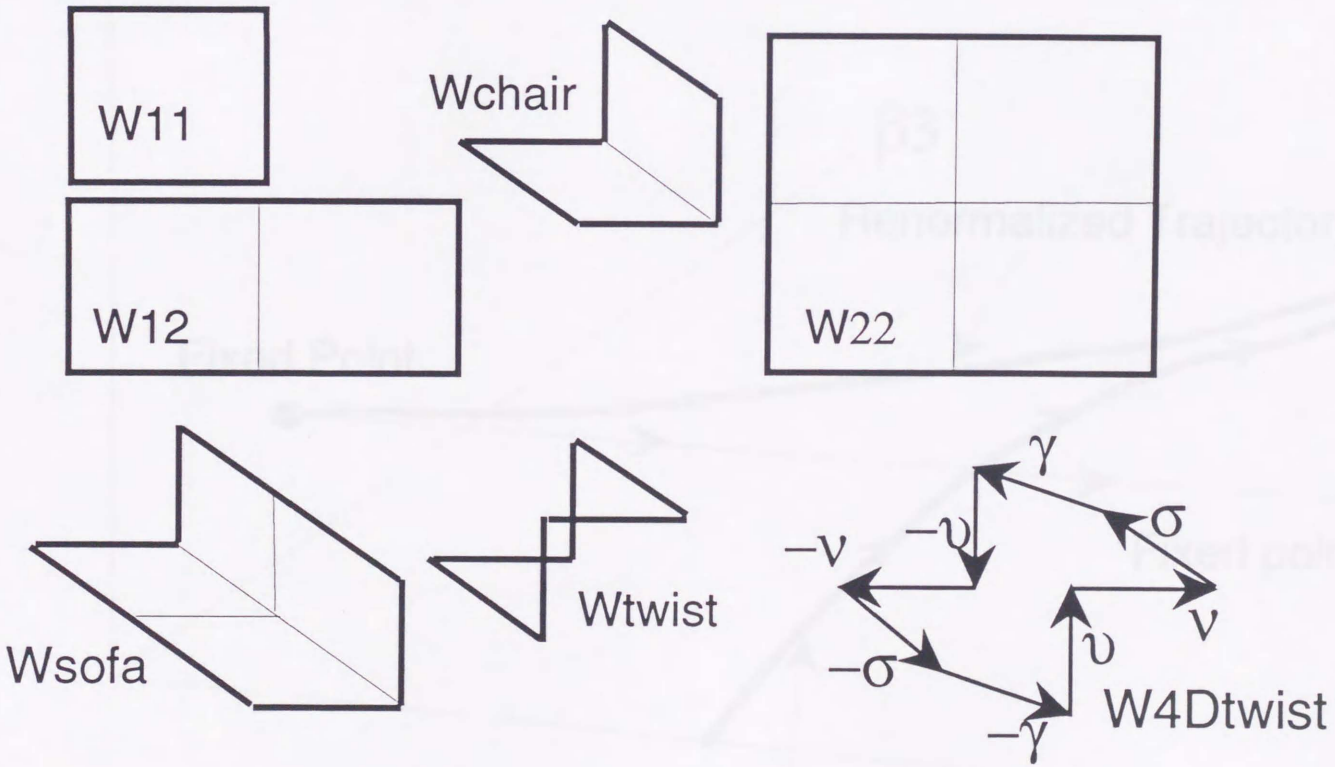

Figure 3

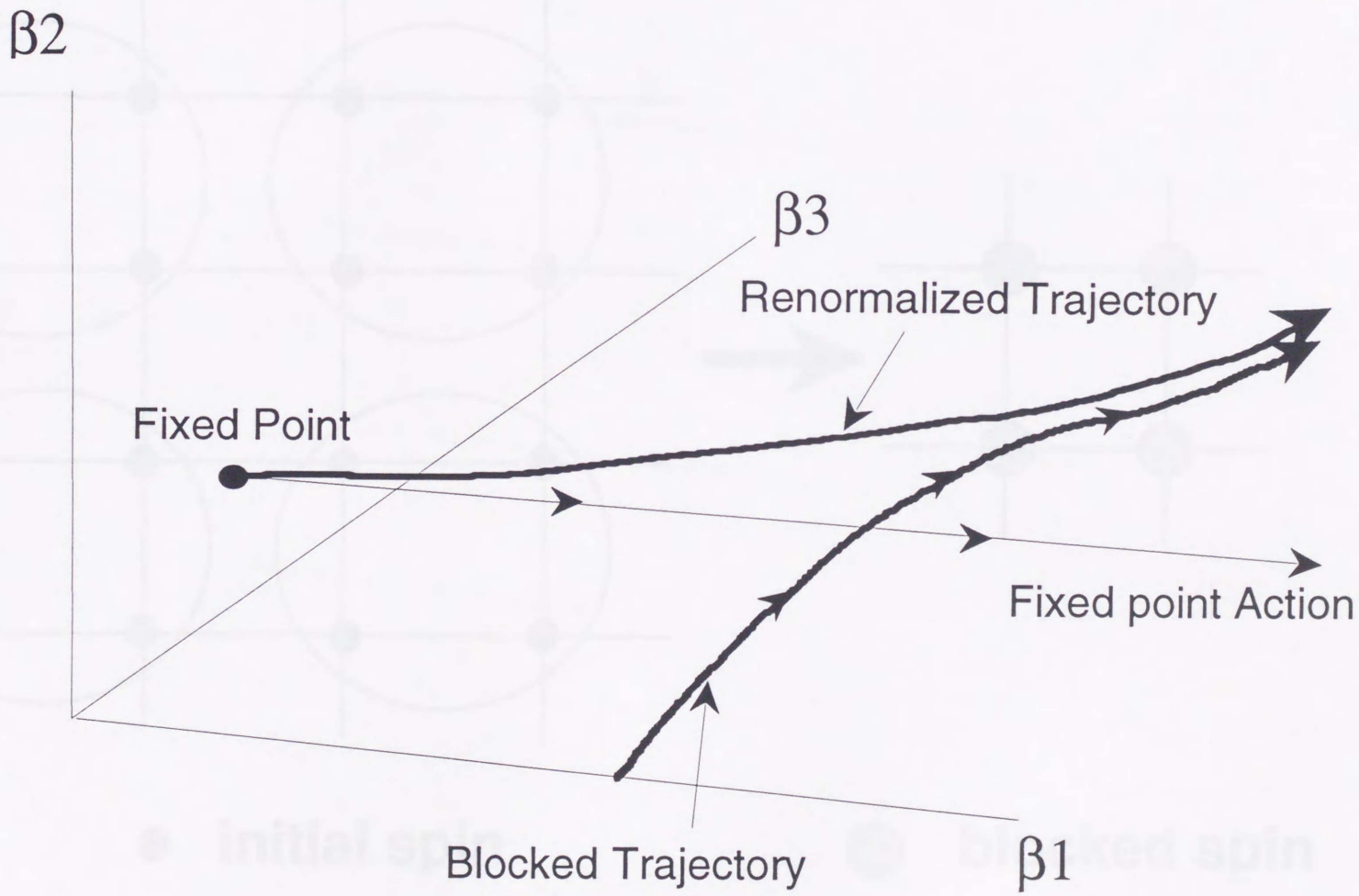
β2
β3
Renormalized Trajectory
Fixed Point
Fixed point Action
Blocked Trajectory
β1

Figure 4

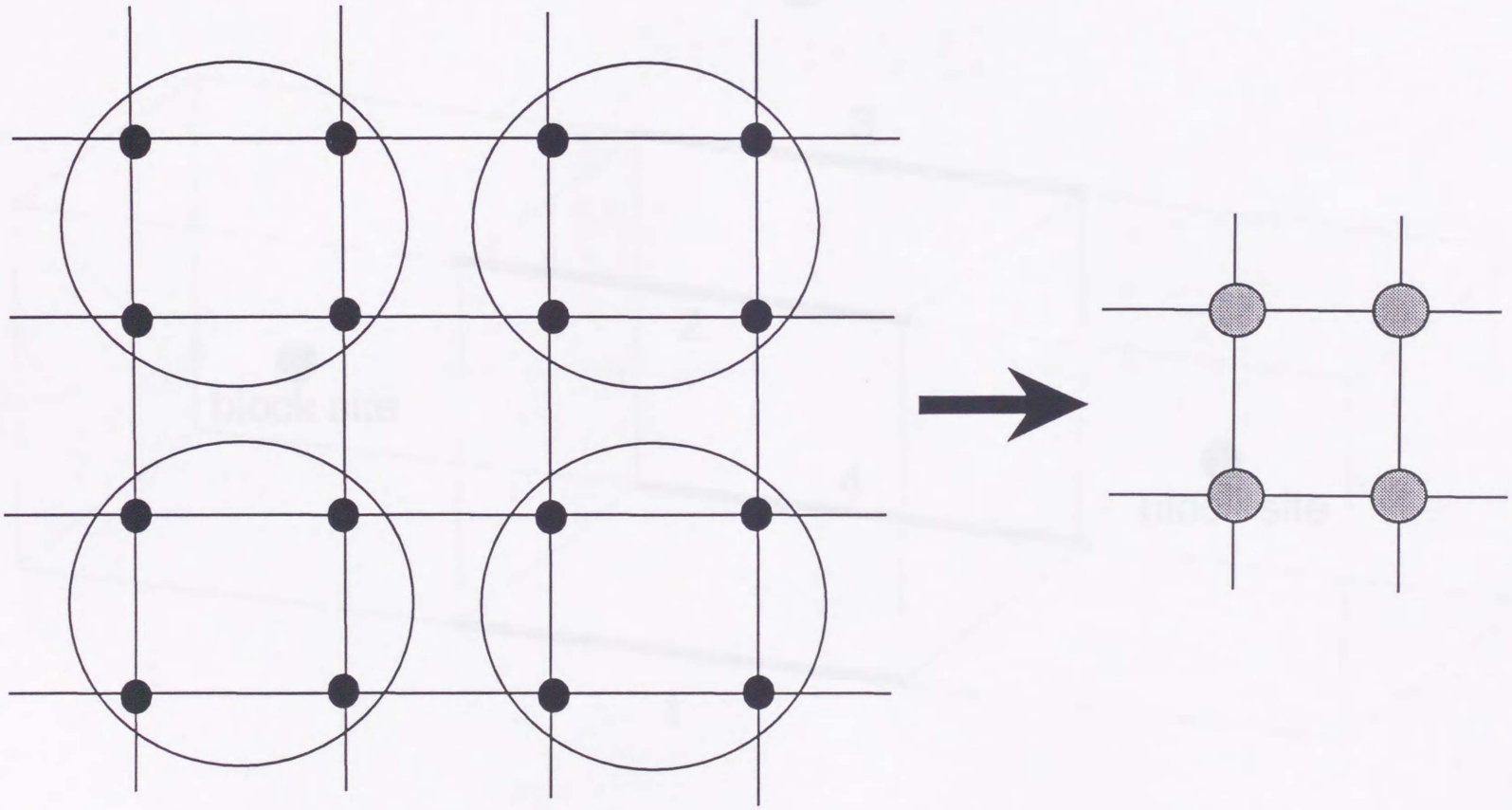

initial spin

blocked spin

Figure 5

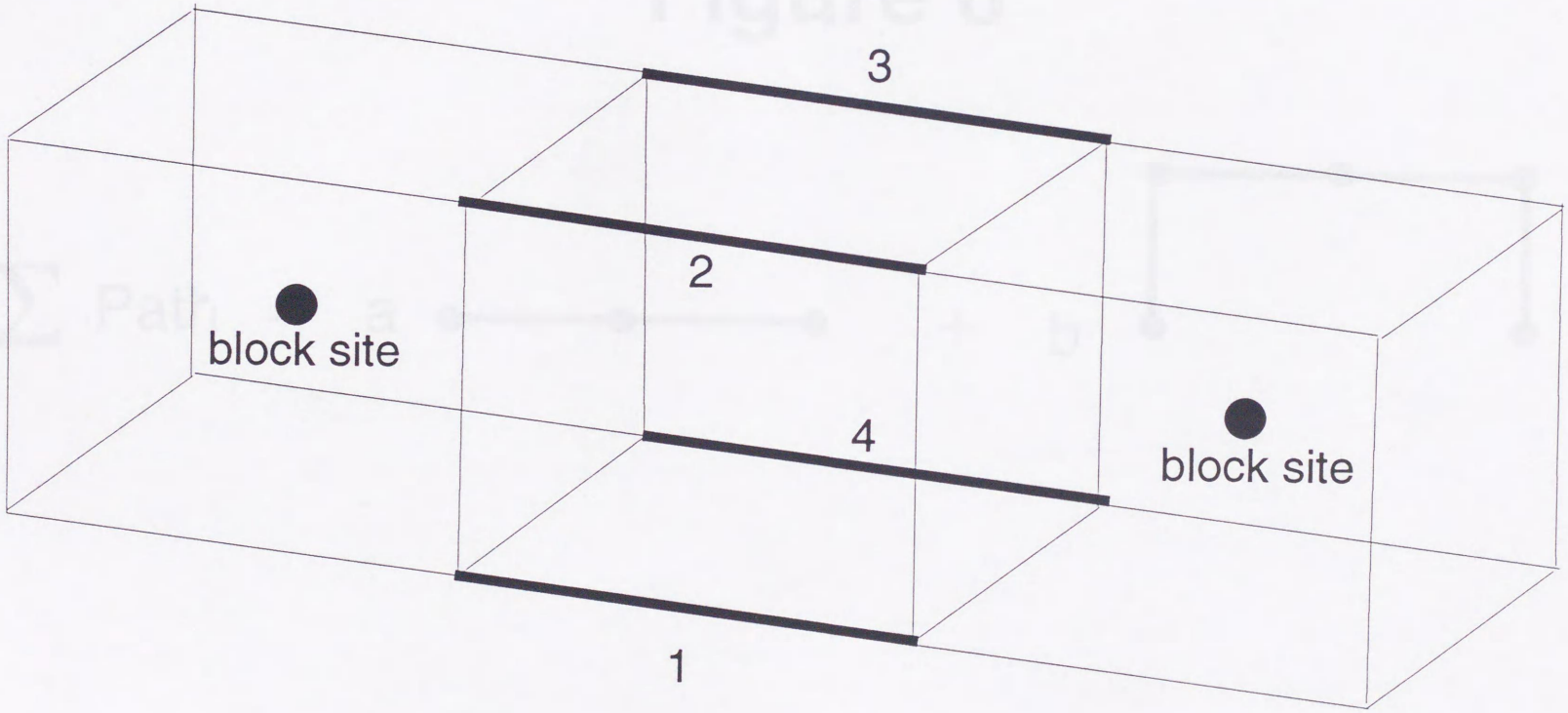

Figure 6

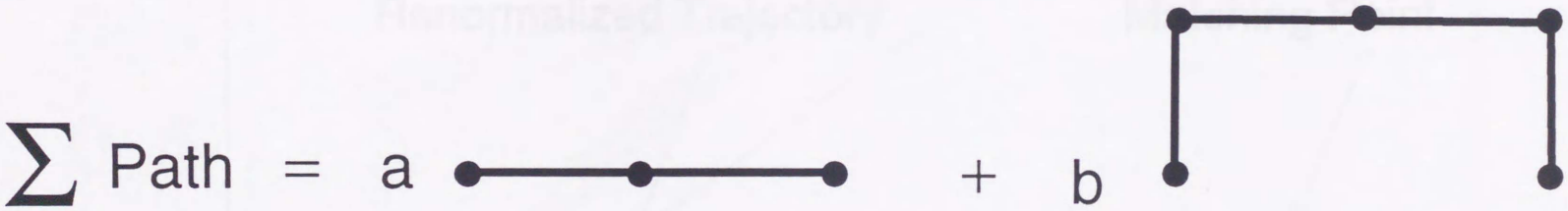

Figure 7

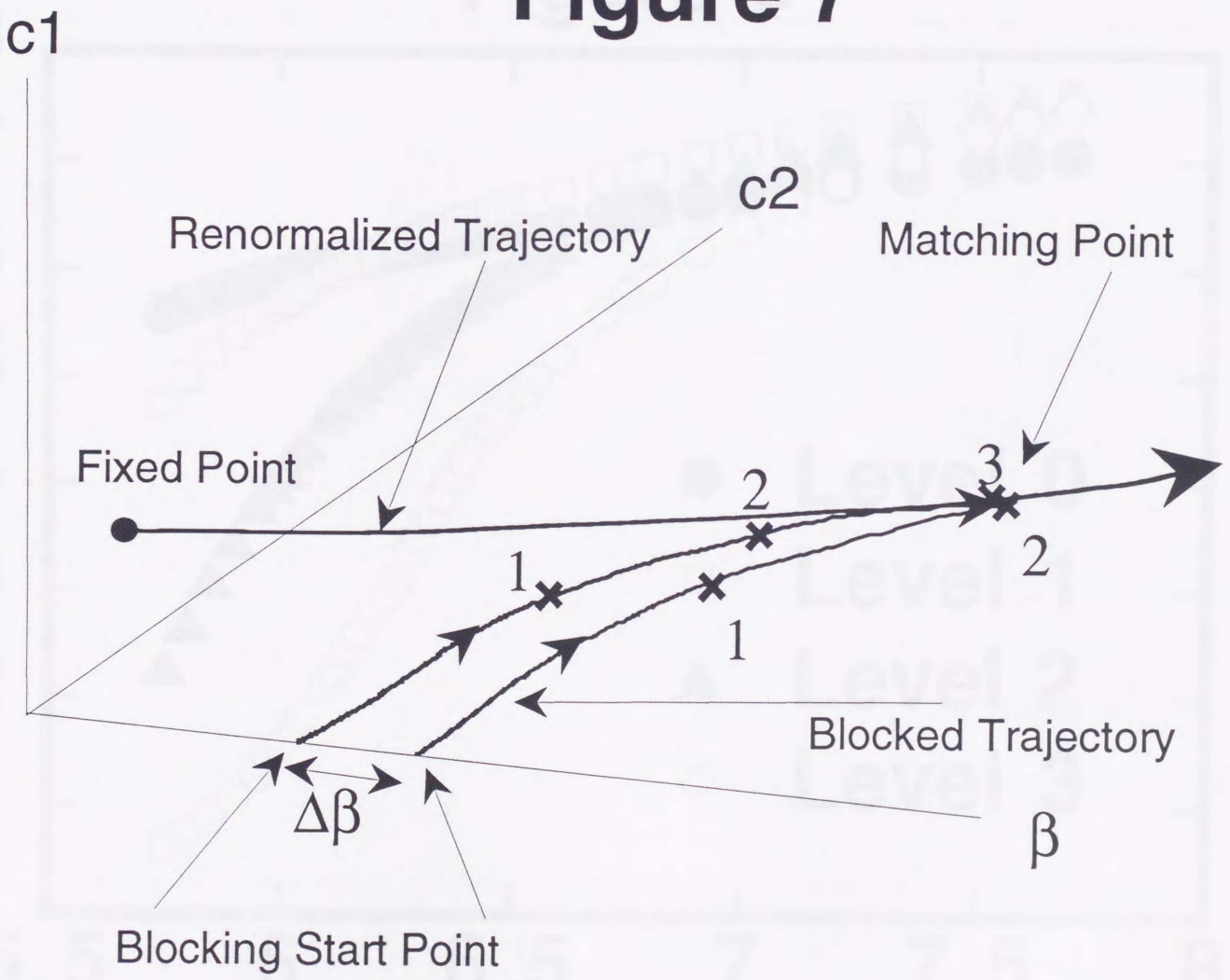
c1
c2
Renormalized Trajectory
Matching Point
Fixed Point
3
2
2
1
1
Blocked Trajectory
Δβ
β
Blocking Start Point

Figure 8

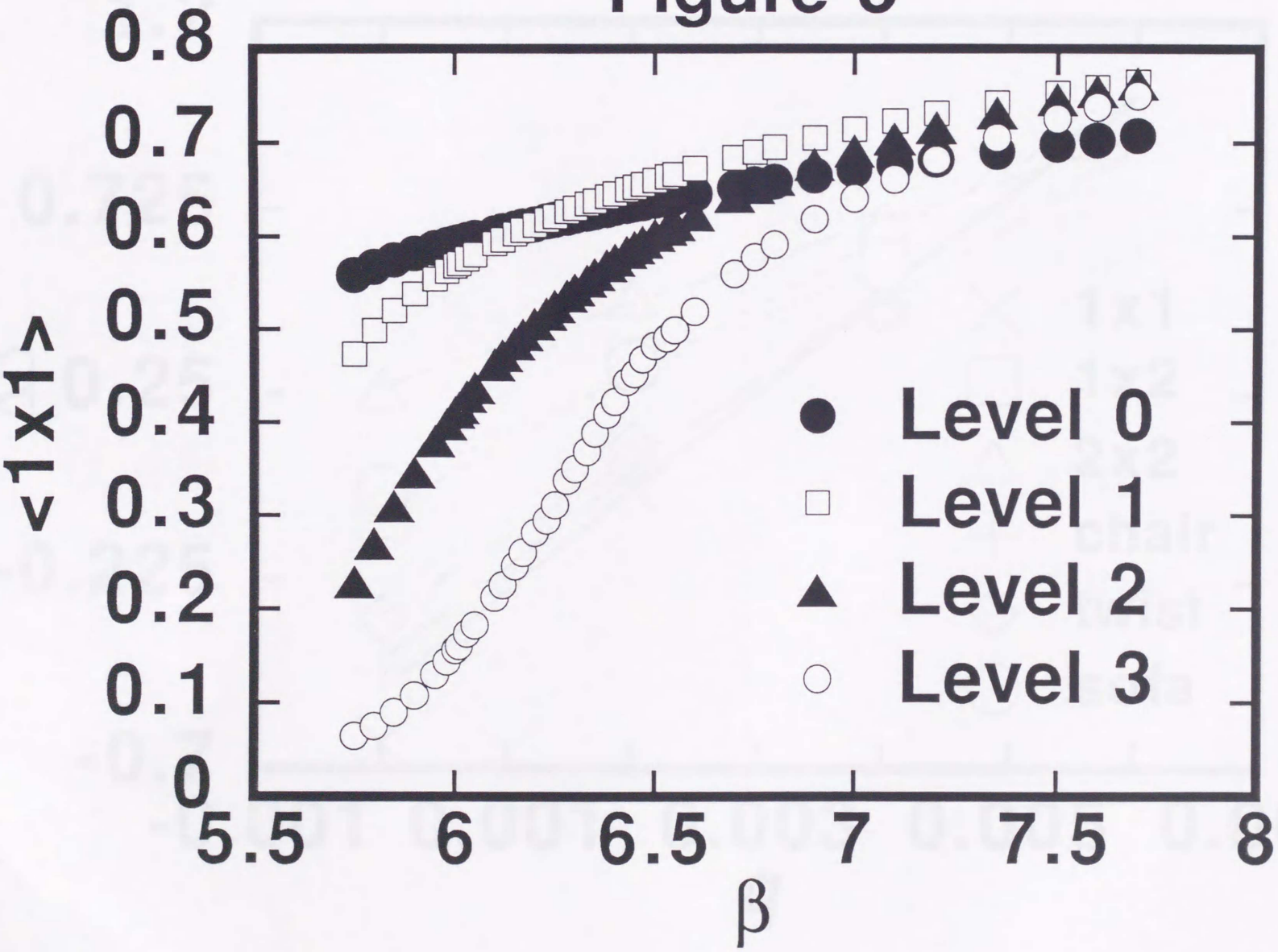
0.8
0.7
0.6
0.5
0.4
0.3
0.2
0.1
0
<1x1>
5.5
6
6.5
7
7.5
8
β
Level 0
Level 1
Level 2
Level 3

Fig.9(a) Level 1

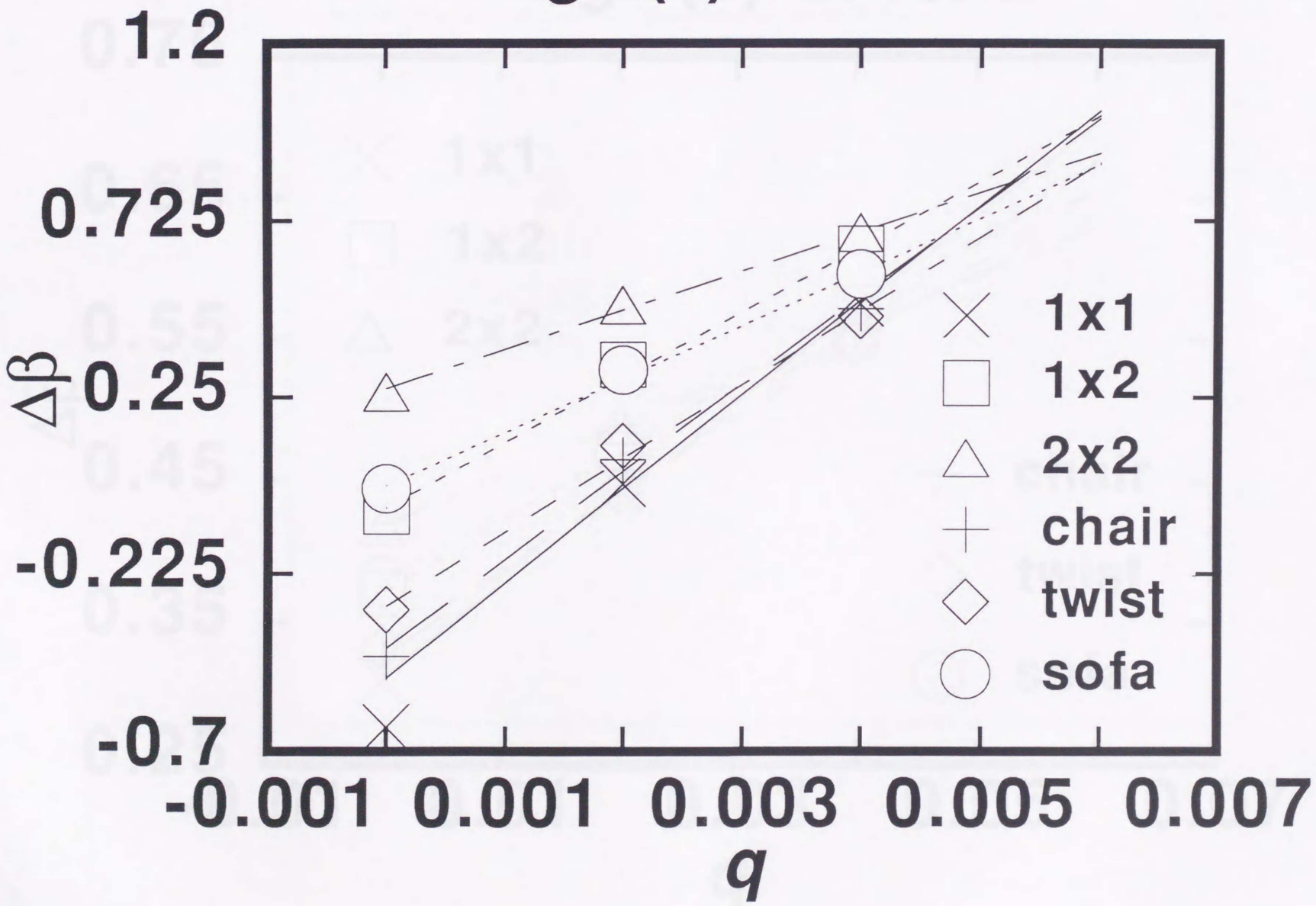

Fig.9(b) Level 2

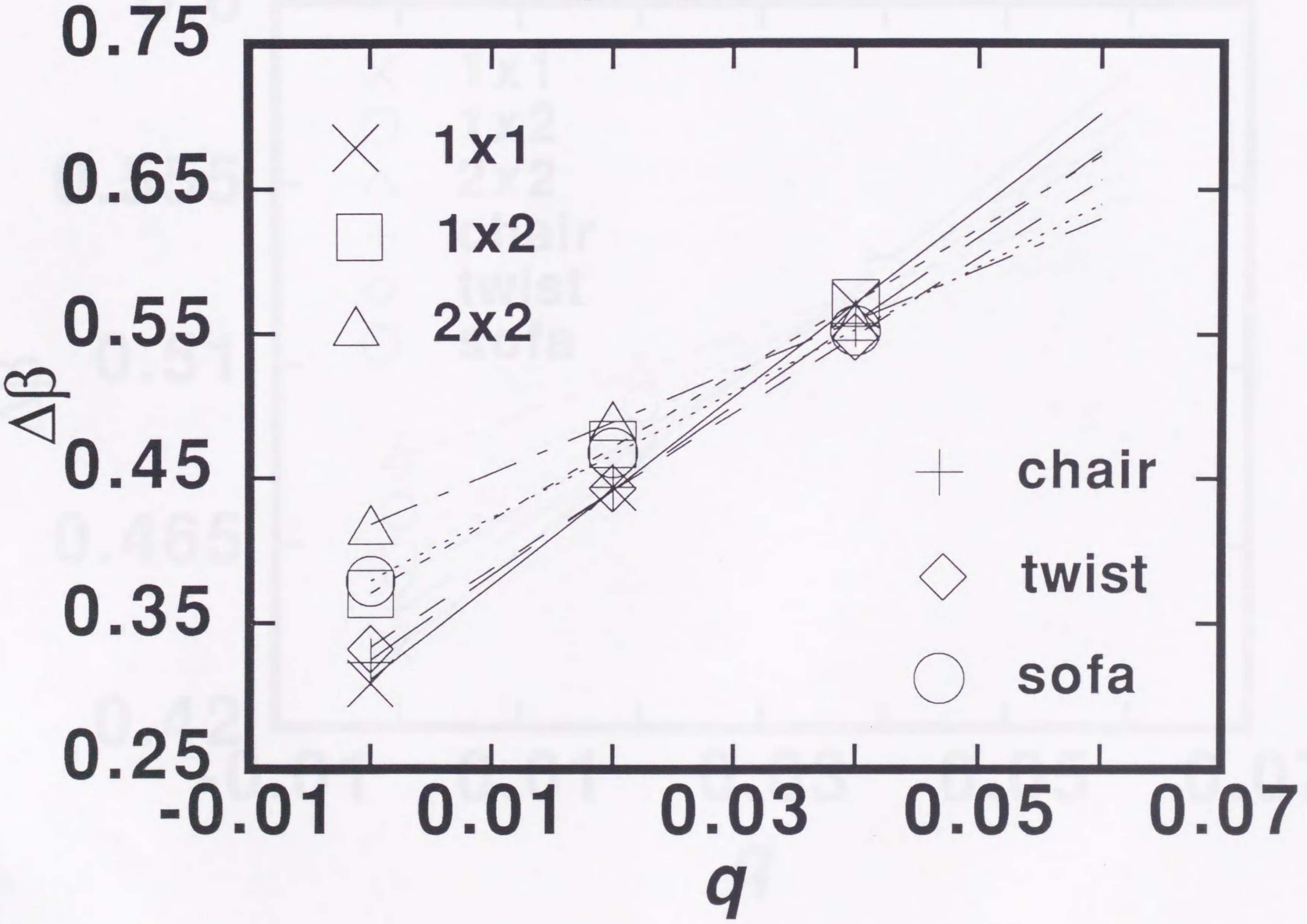

Fig.9(c) level 3

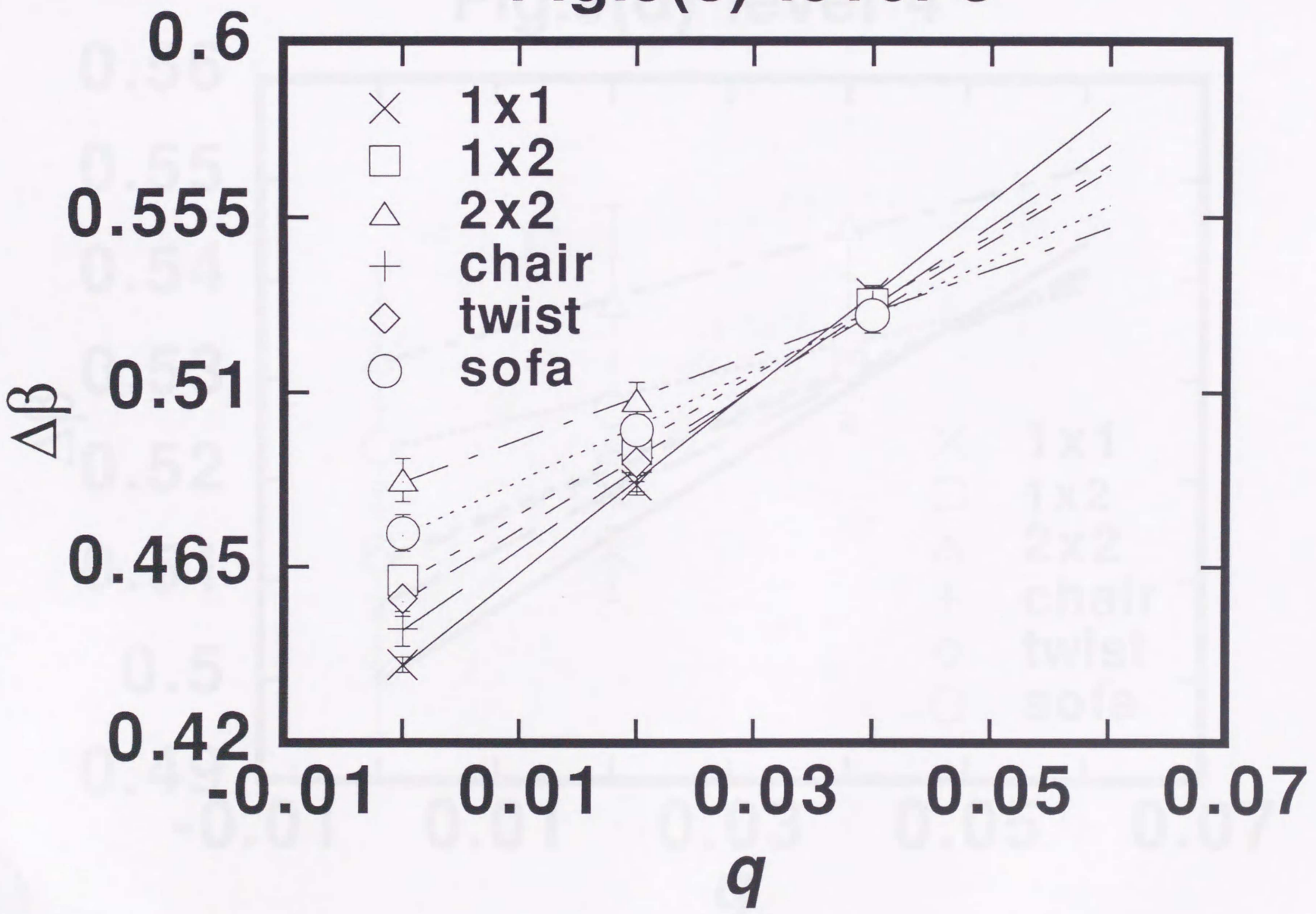

Fig.9(d) level 4

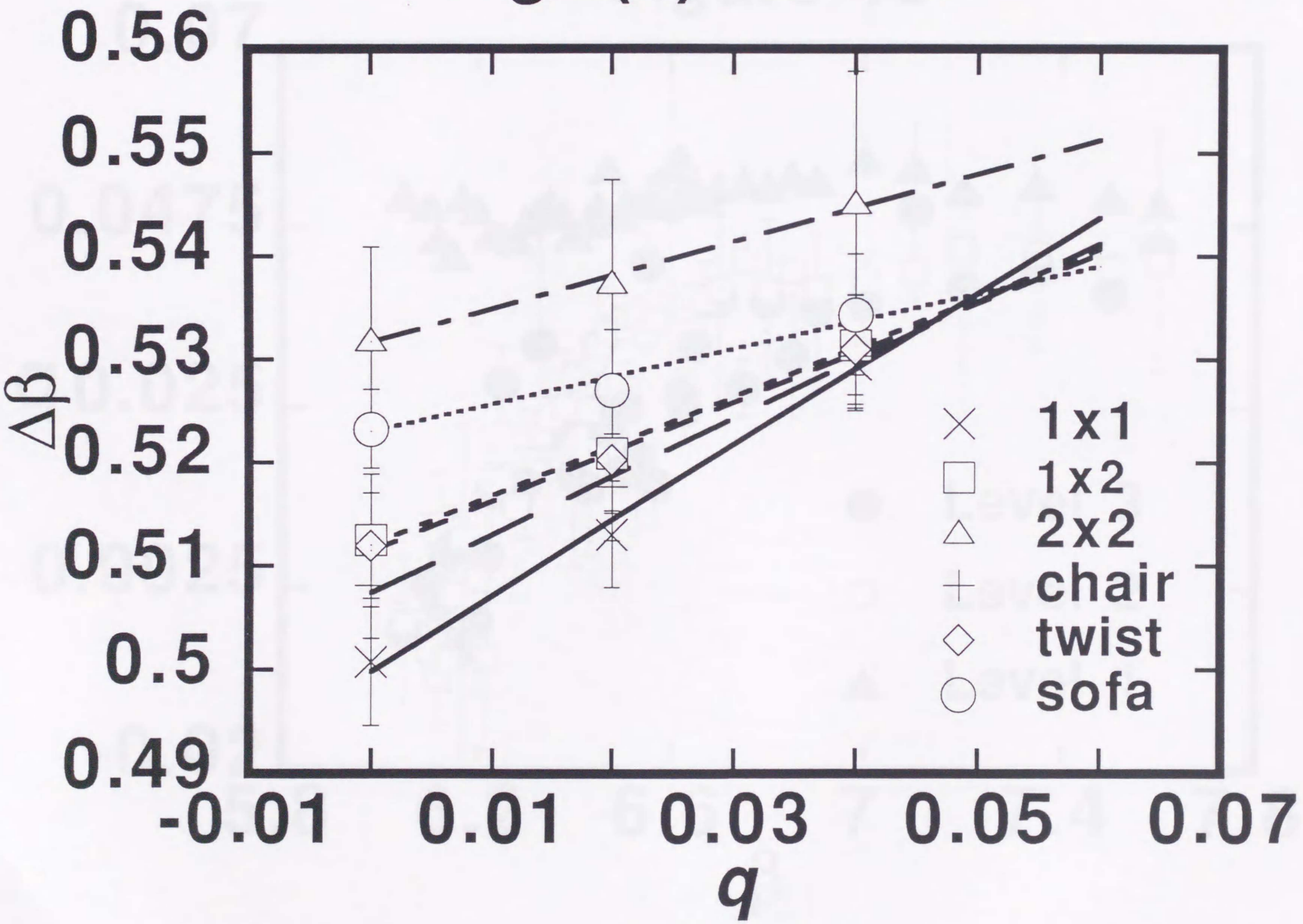

Figure 10

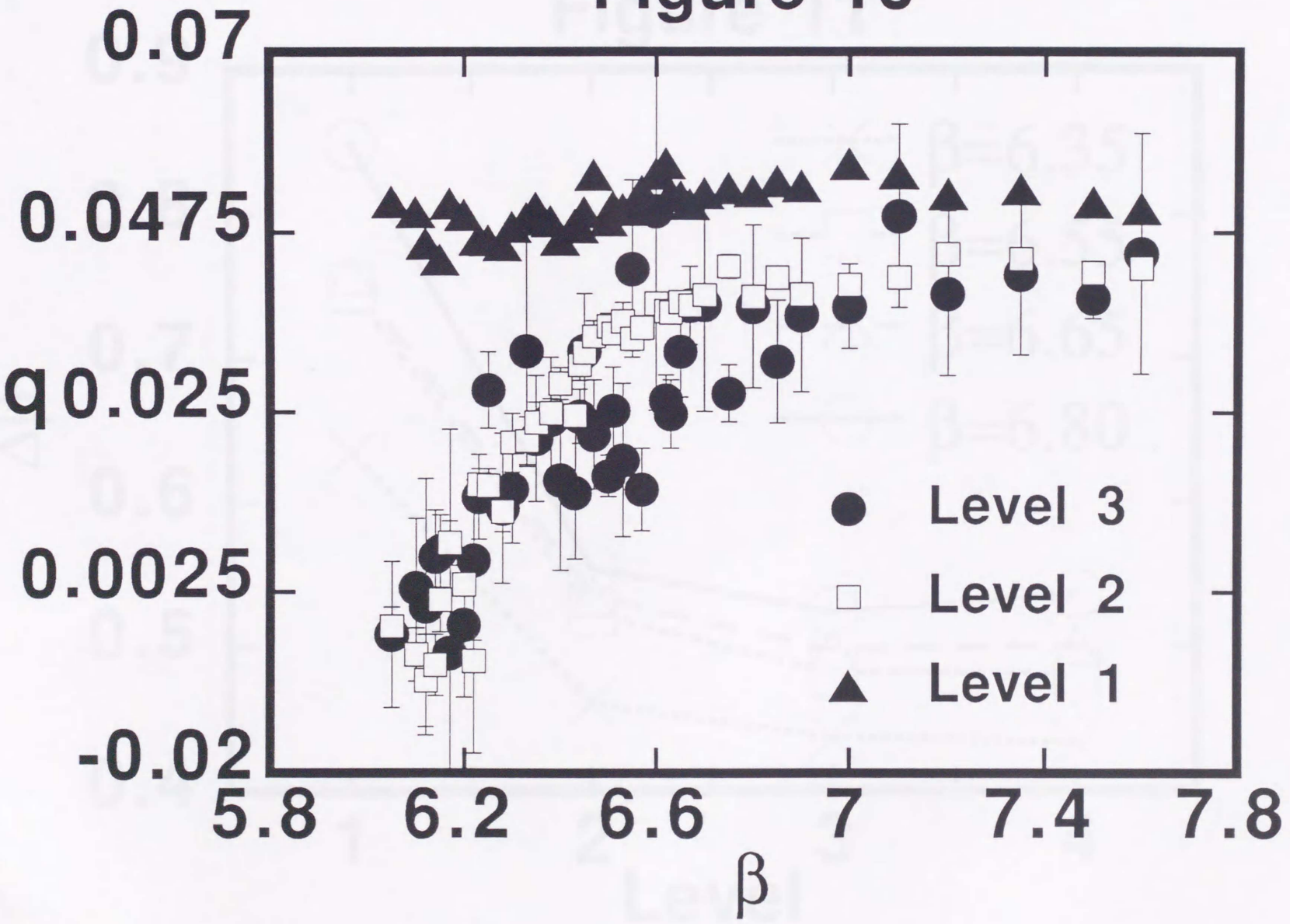
0.07
0.0475
q 0.025
0.0025
-0.02
5.8
6.2
6.6
7
7.4
7.8
β
Level 3
Level 2
Level 1

Figure 11

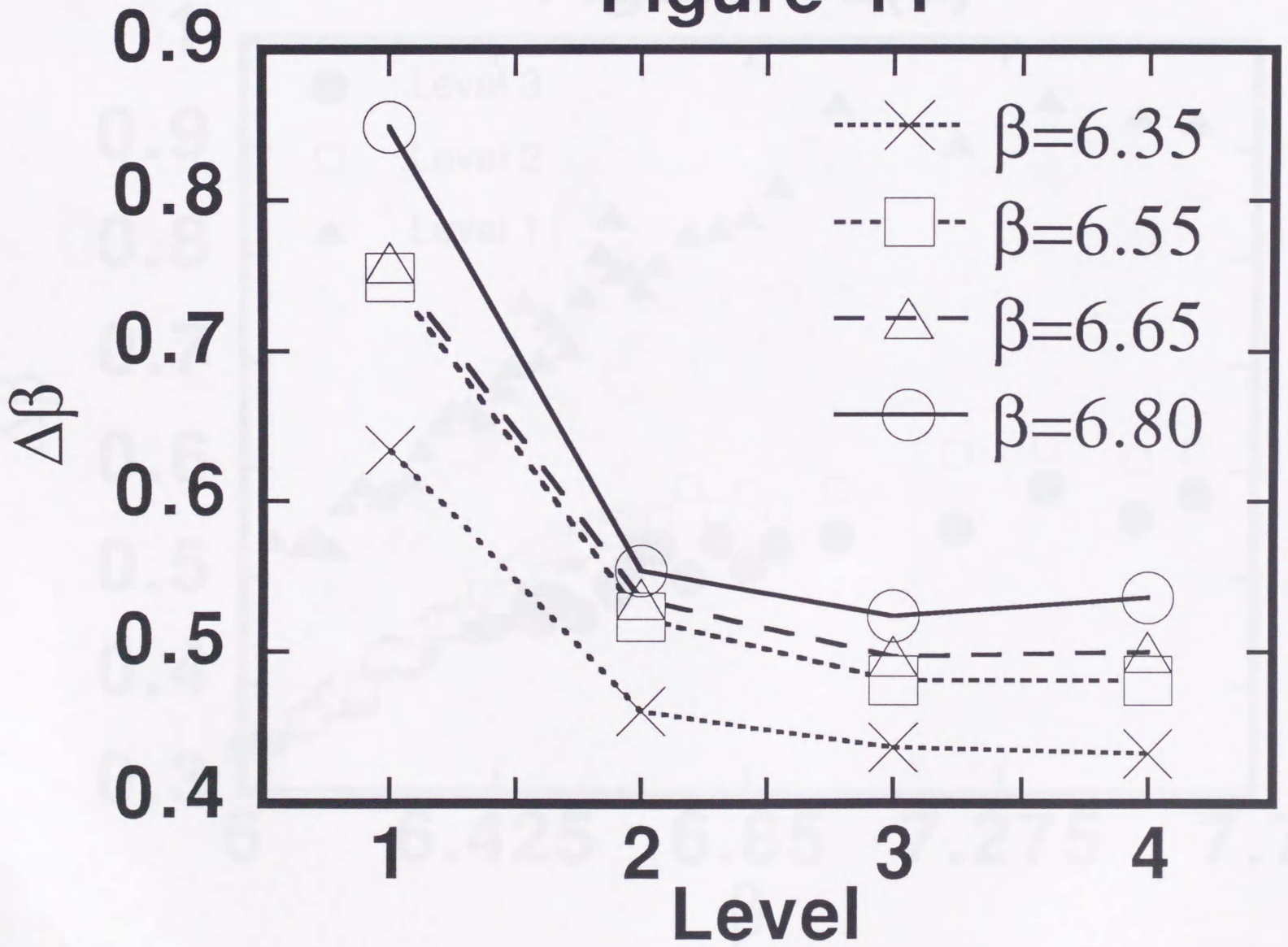

Figure 12(a)

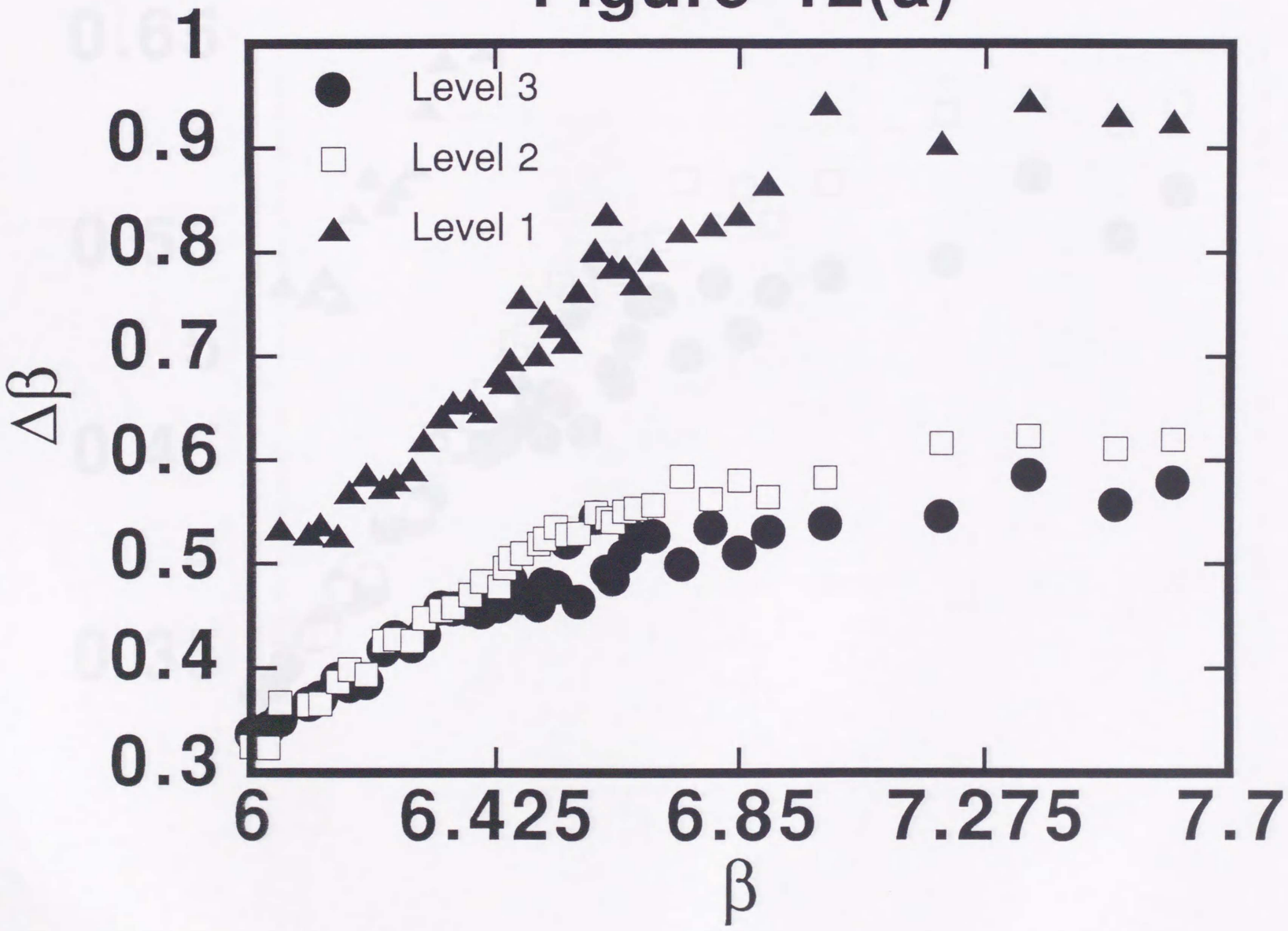
Level 3
Level 2
Level 1
Δβ
1
0.9
0.8
0.7
0.6
0.5
0.4
0.3
6
6.425
6.85
7.275
7.7
β

Figure 12(b)

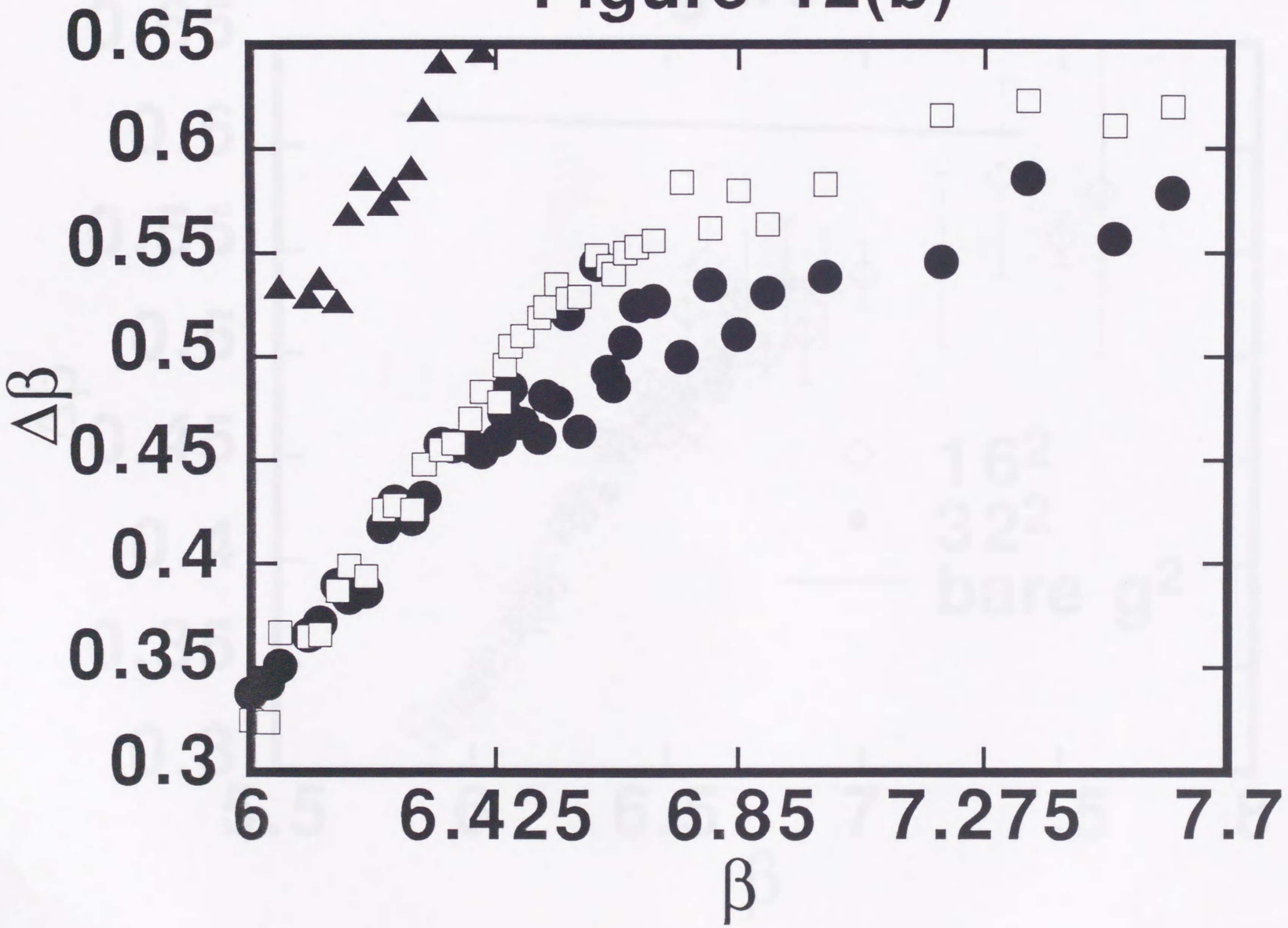

Figure 13

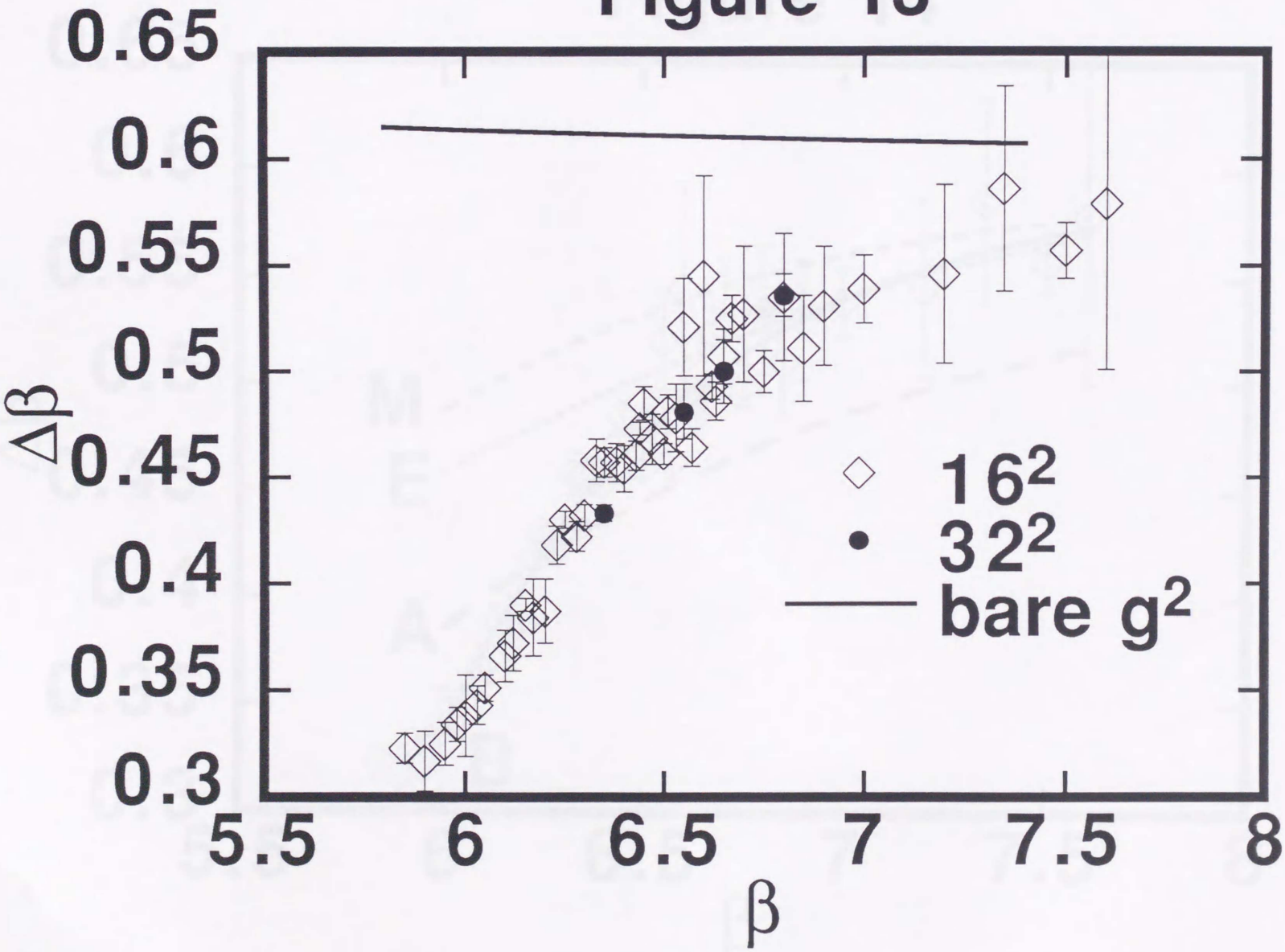

Figure 14

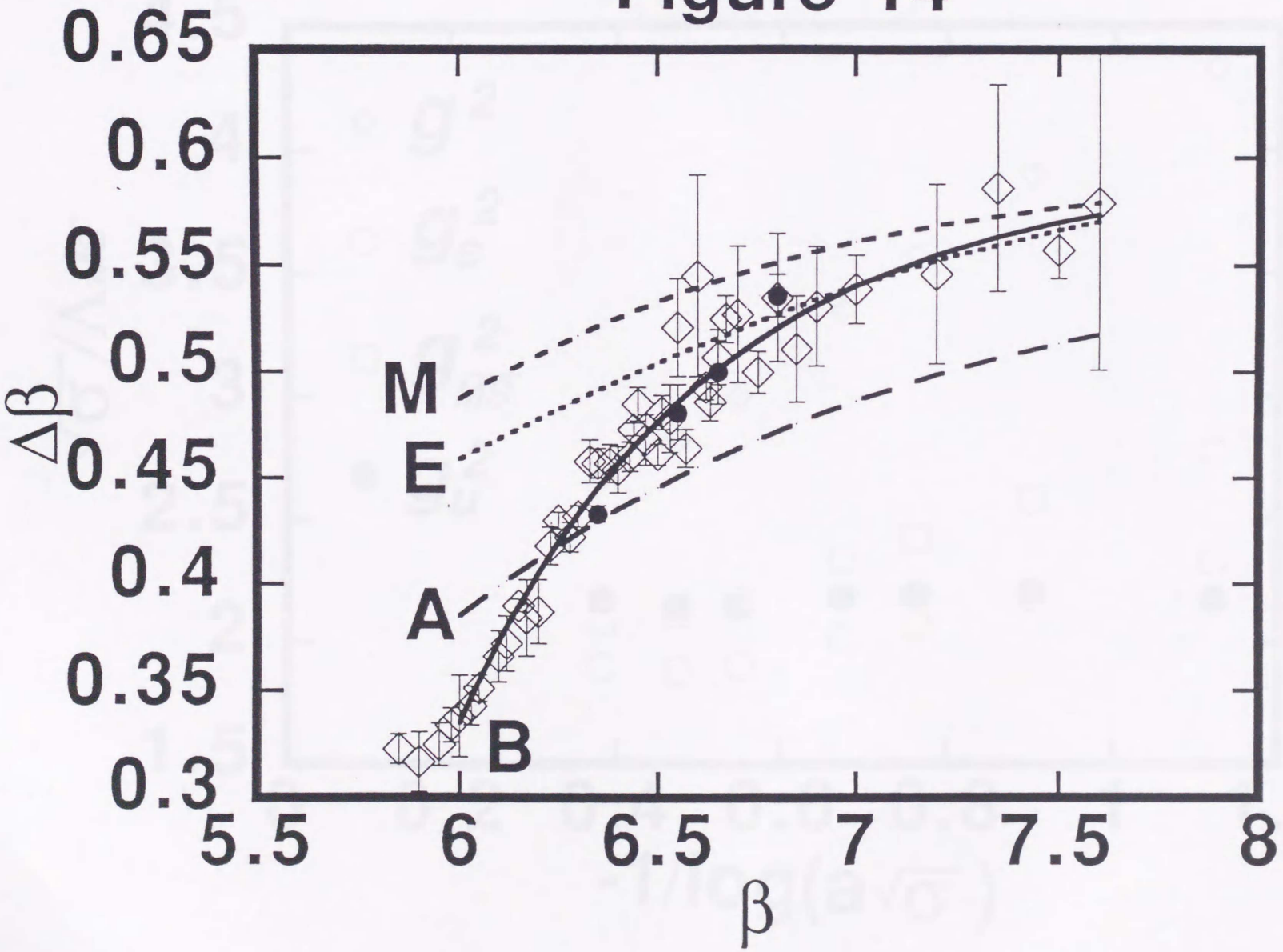

Figure 15

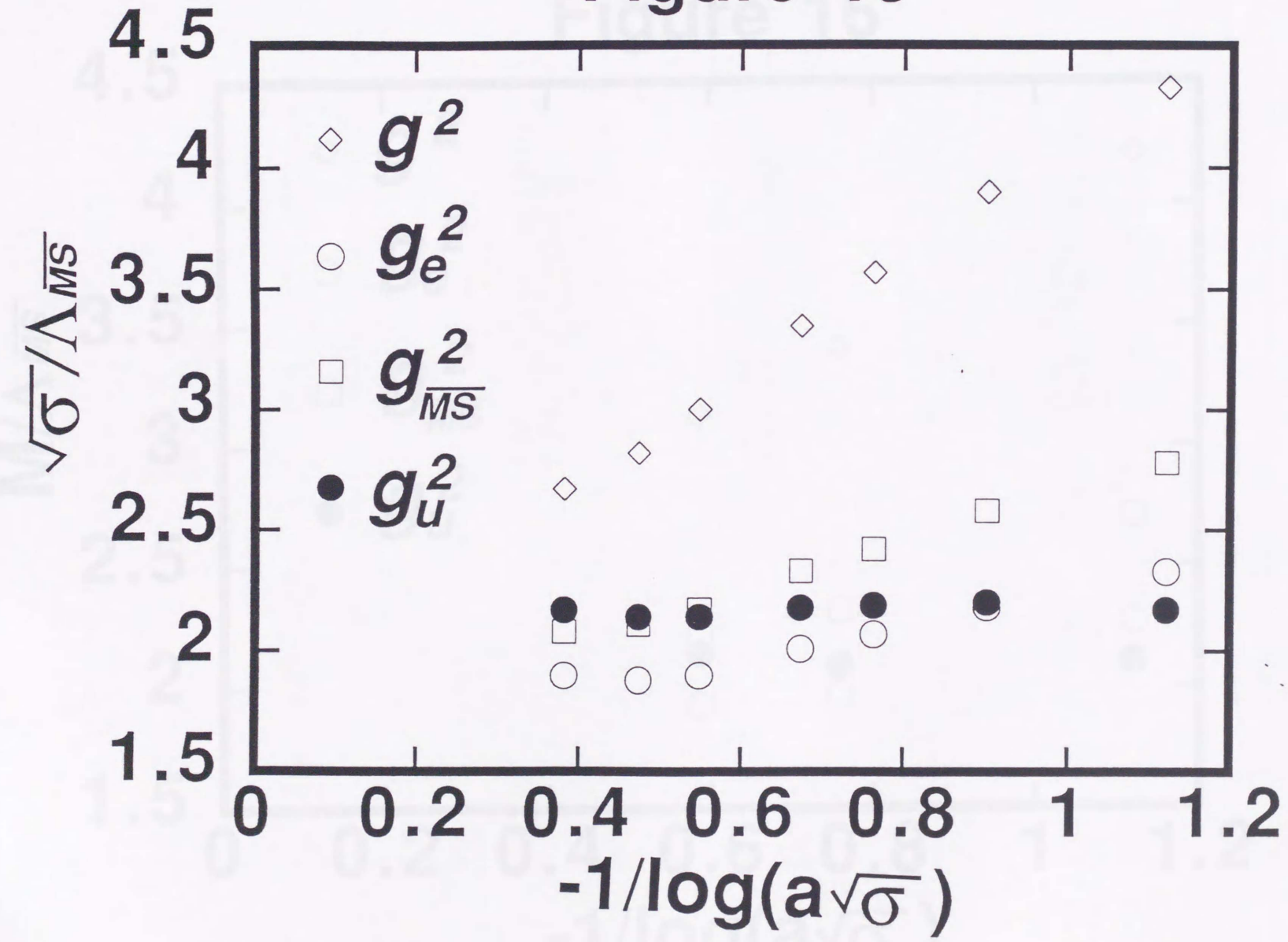
4.5
4
3.5
3
2.5
2
1.5
0
0.2
0.4
0.6
0.8
1
1.2
g^2
g_e^2
$g_{\overline{MS}}^2$
g_u^2
$\sqrt{\sigma}/\Lambda_{\overline{MS}}$
$-1/\log(a\sqrt{\sigma})$

Figure 16

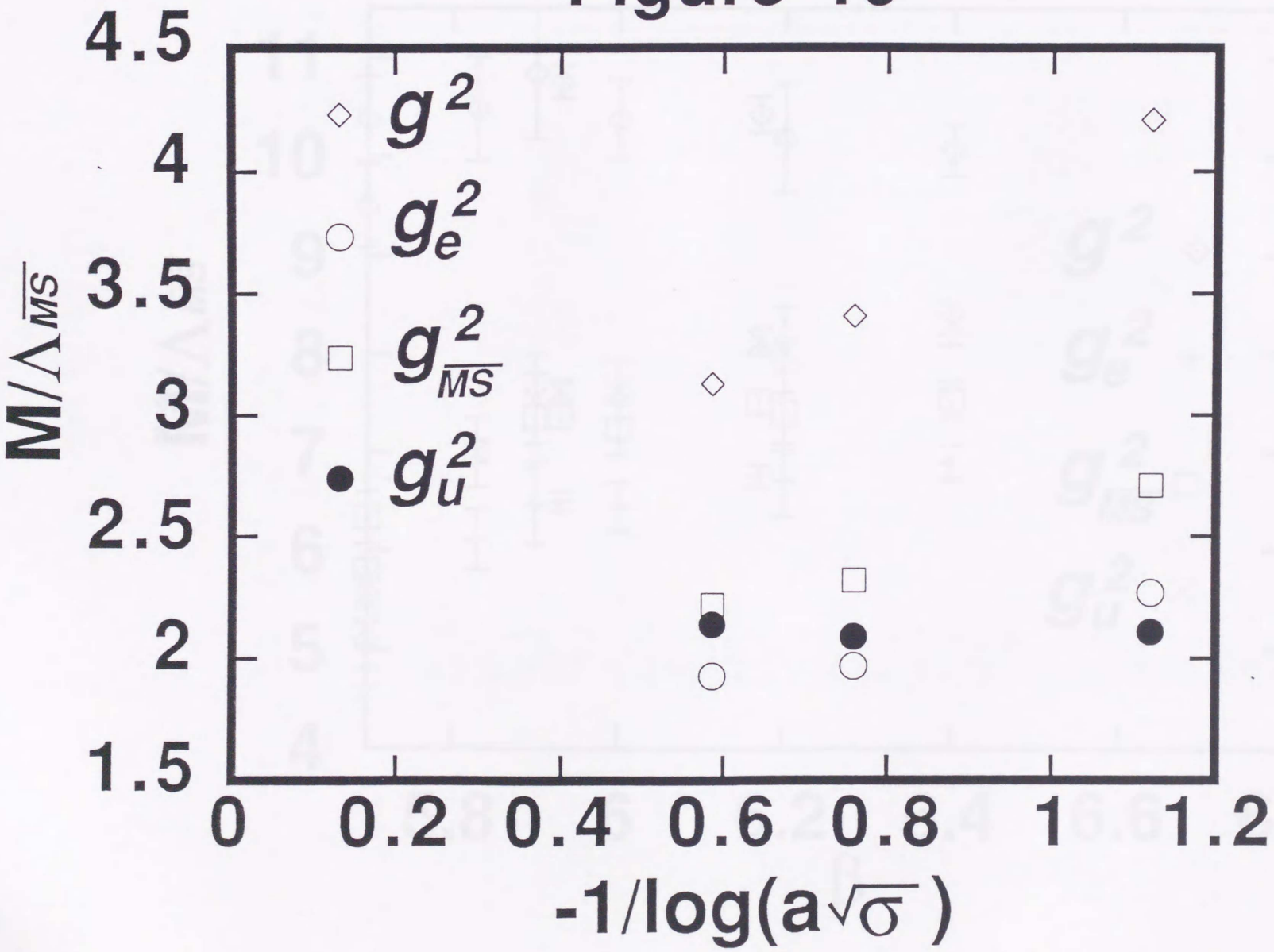
4.5
4
3.5
3
2.5
2
1.5
0
0.2
0.4
0.6
0.8
1
1.2
$M/\Lambda_{\overline{MS}}$
g^2
g_e^2
$g^2_{\overline{MS}}$
g_u^2
$-1/\log(a\sqrt{\sigma})$

Figure 17

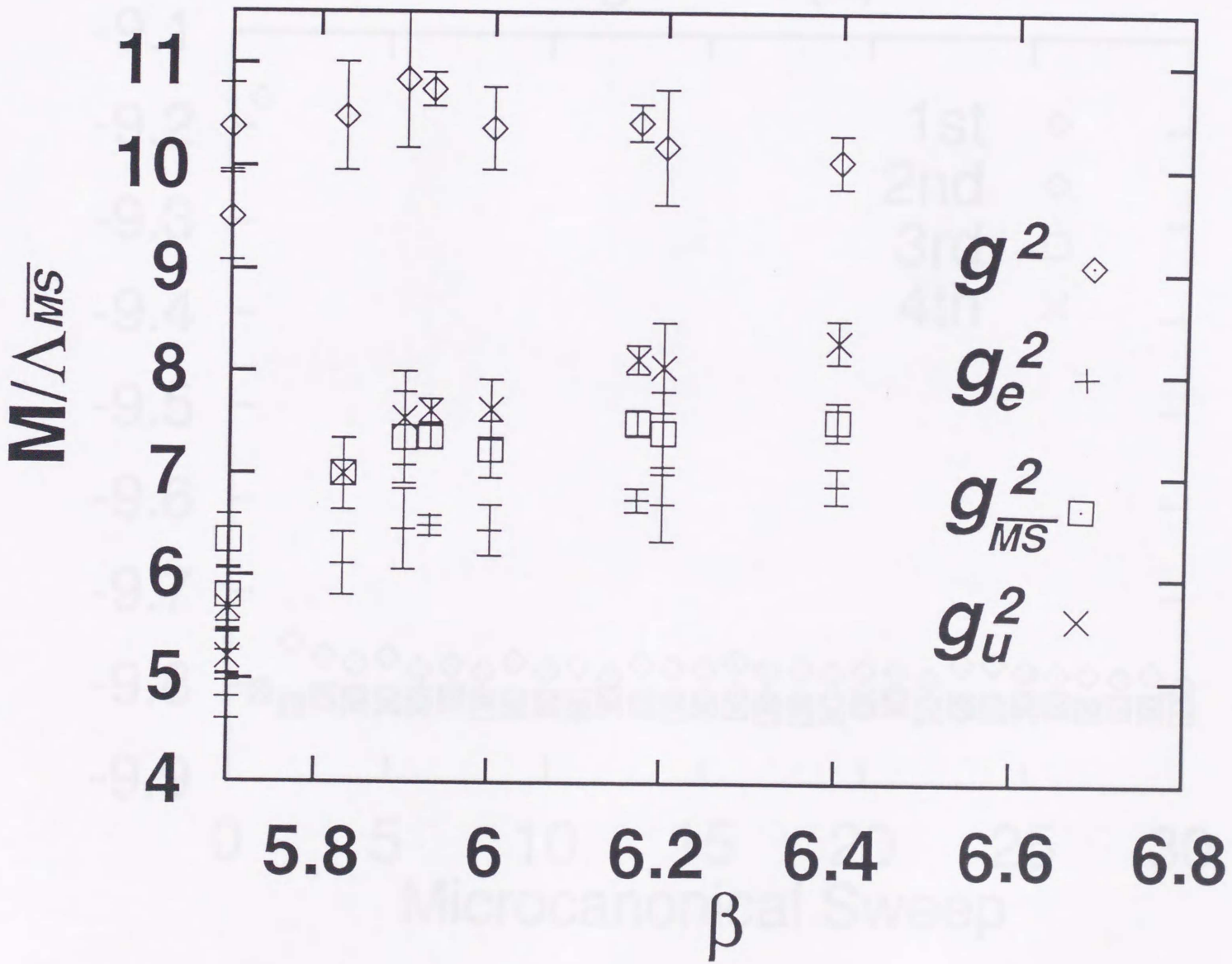

Figure 18(a)

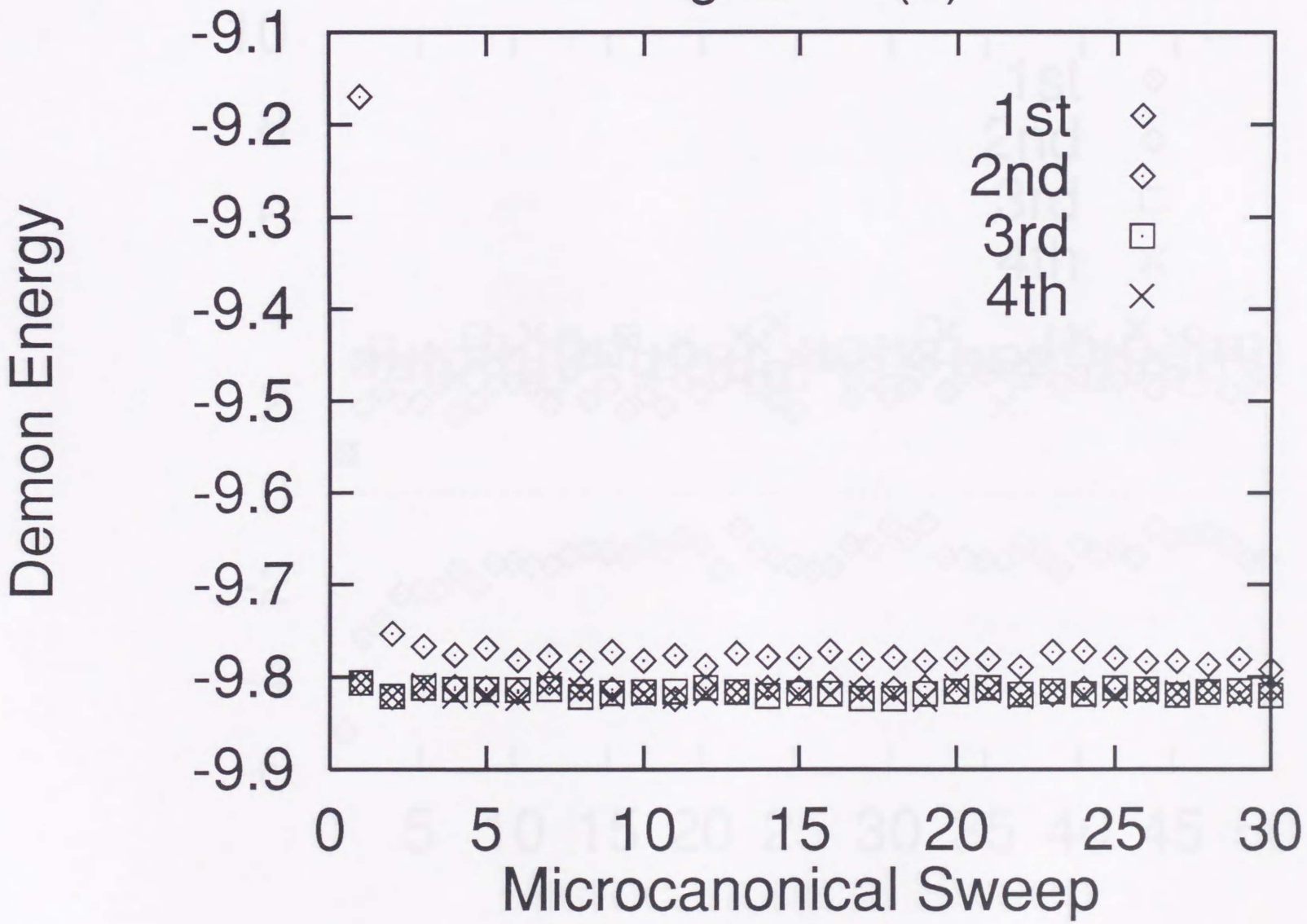
-9.1
-9.2
-9.3
-9.4
-9.5
-9.6
-9.7
-9.8
-9.9
Demon Energy
1st
2nd
3rd
4th
0
5
10
15
20
25
30
Microcanonical Sweep

Figure 18(b)

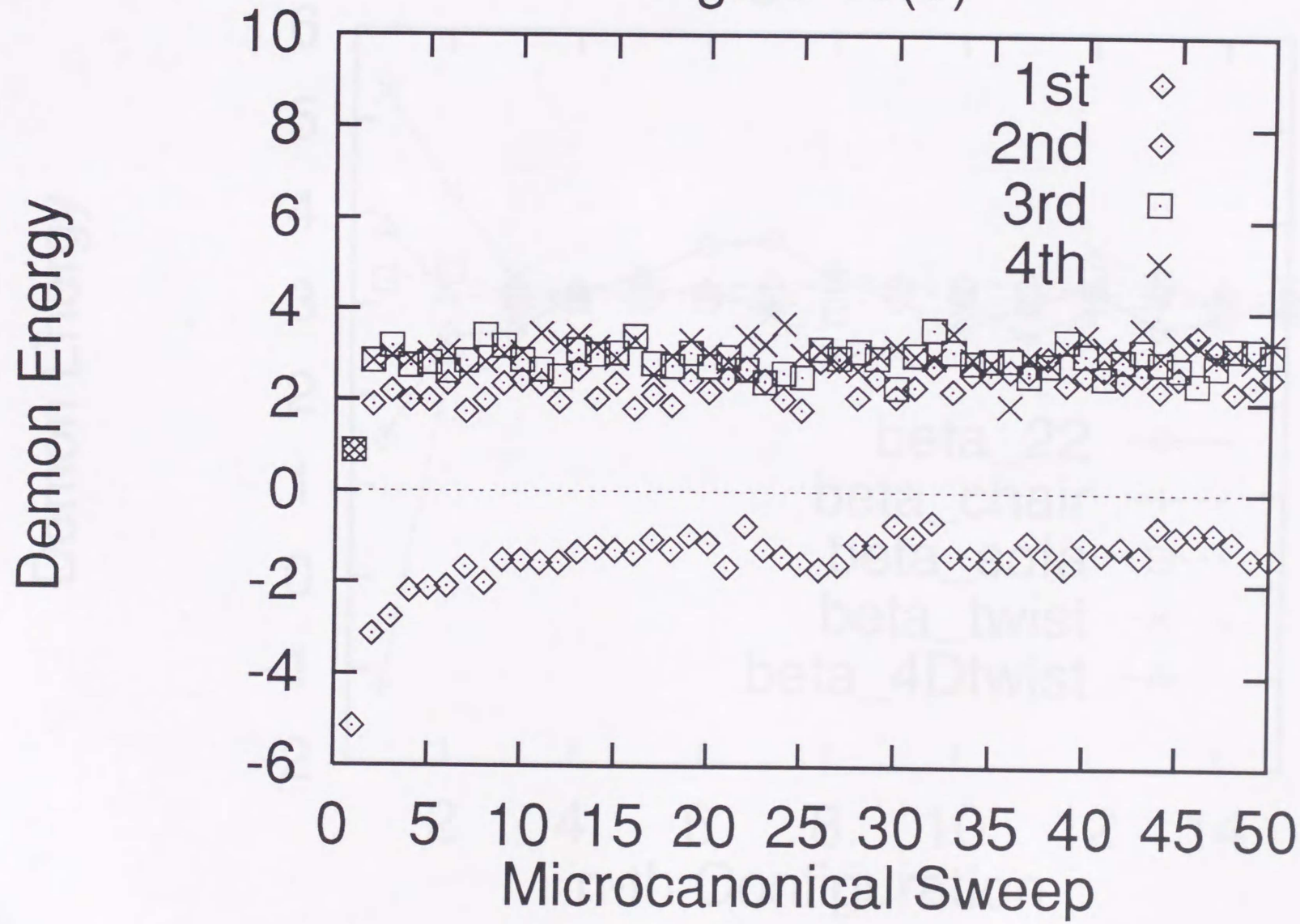
Demon Energy
10
8
6
4
2
0
-2
-4
-6
0
5
10
15
20
25
30
35
40
45
50
Microcanonical Sweep
1st
2nd
3rd
4th

Figure 19

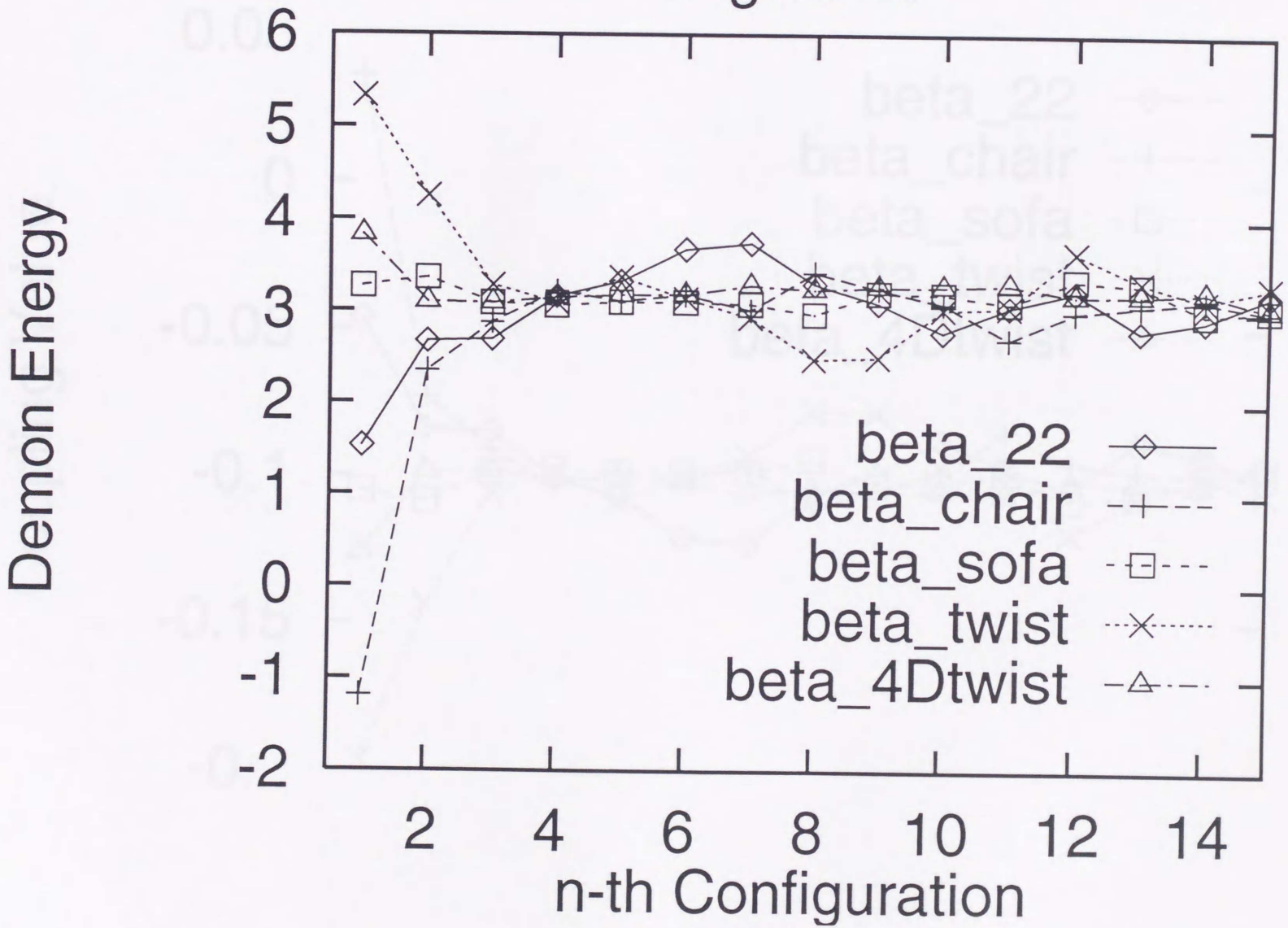
Demon Energy
6
5
4
3
2
1
0
-1
-2
2
4
6
8
10
12
14
n-th Configuration
beta_22
beta_chair
beta_sofa
beta_twist
beta_4Dtwist

Figure 20

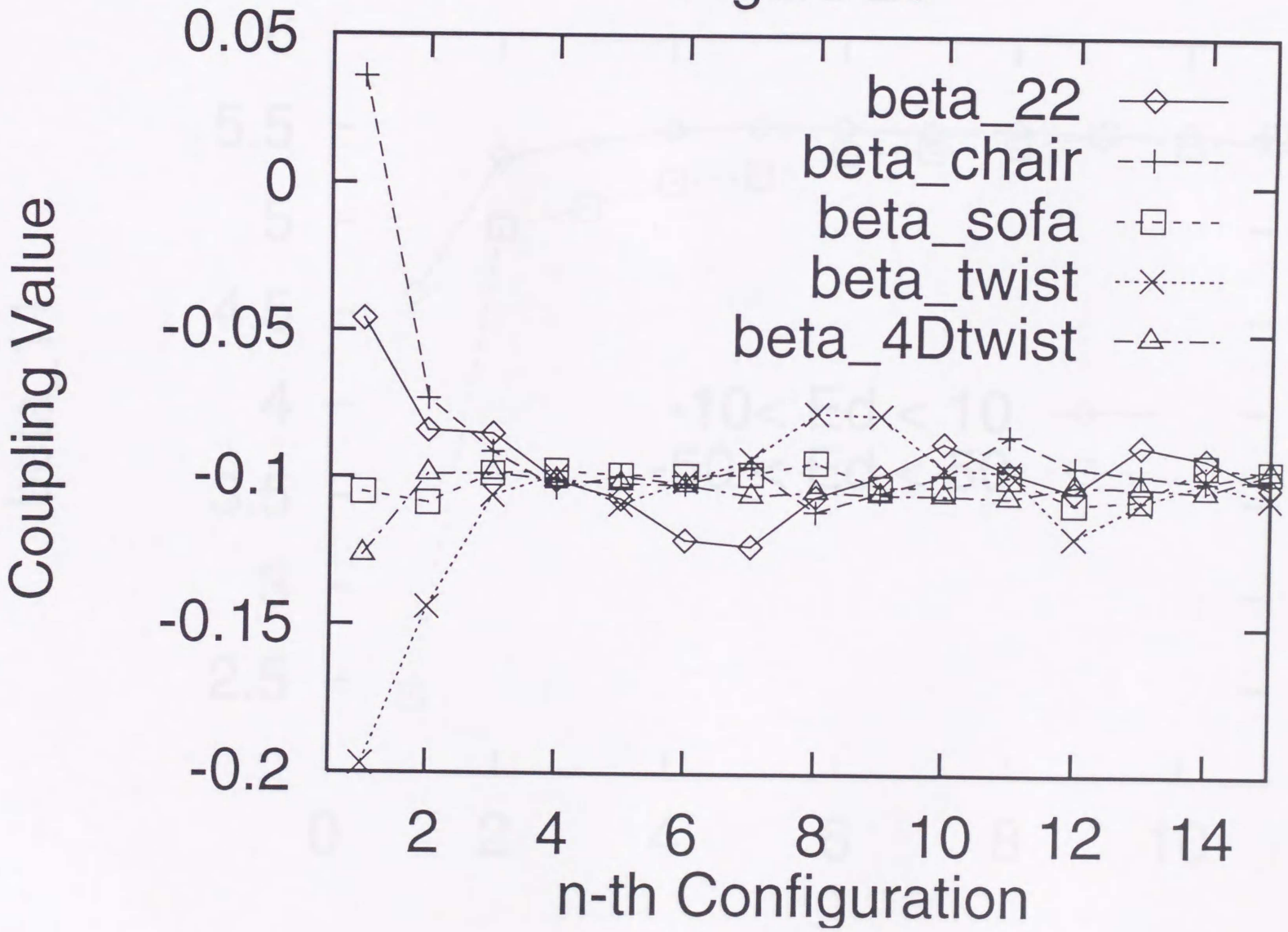
0.05
0
-0.05
-0.1
-0.15
-0.2
Coupling Value
2
4
6
8
10
12
14
n-th Configuration
beta_22
beta_chair
beta_sofa
beta_twist
beta_4Dtwist

Figure 21

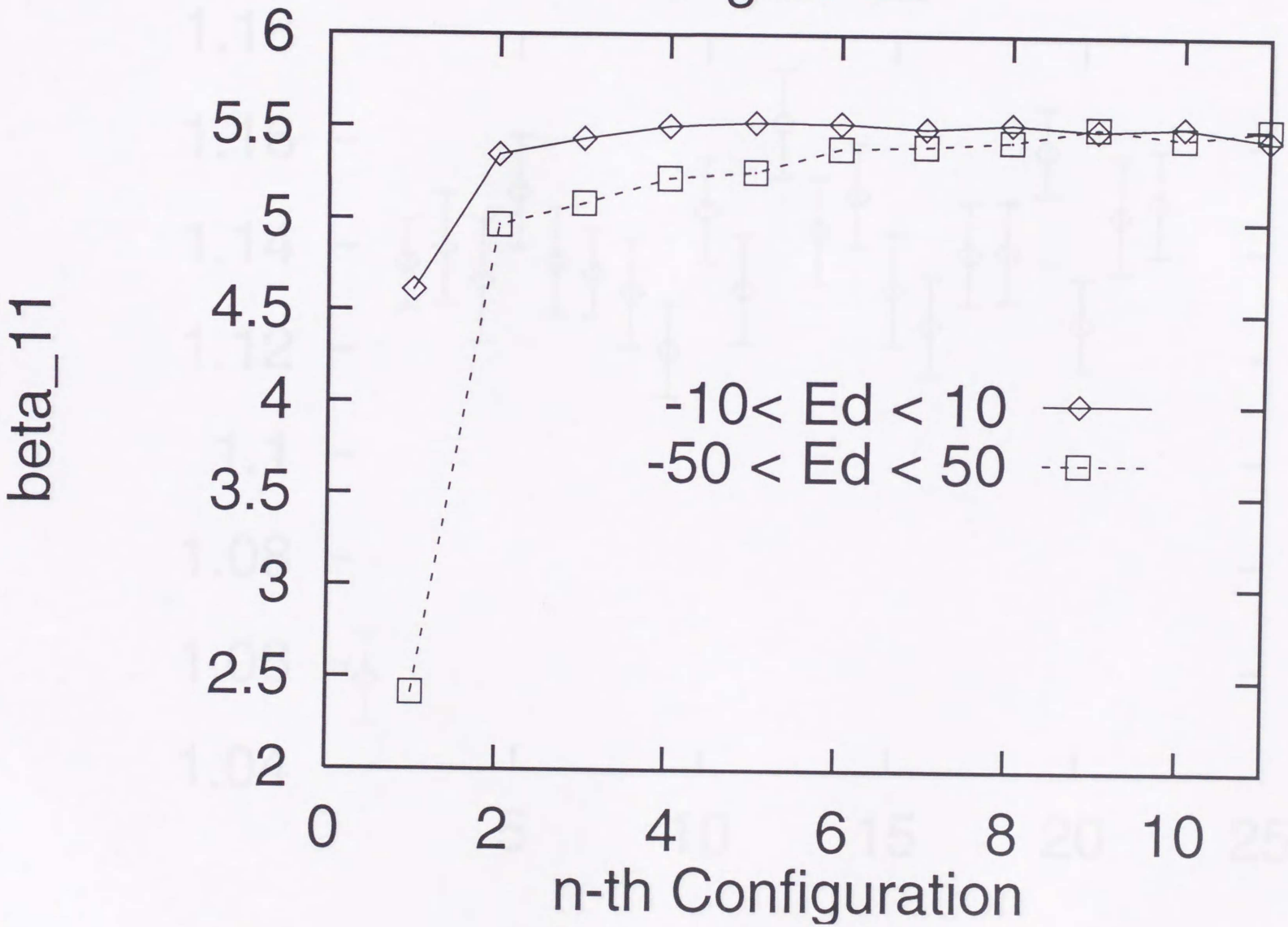
beta_11
6
5.5
5
4.5
4
3.5
3
2.5
2
0
2
4
6
8
10
n-th Configuration
-10< Ed < 10
-50 < Ed < 50

Figure 22

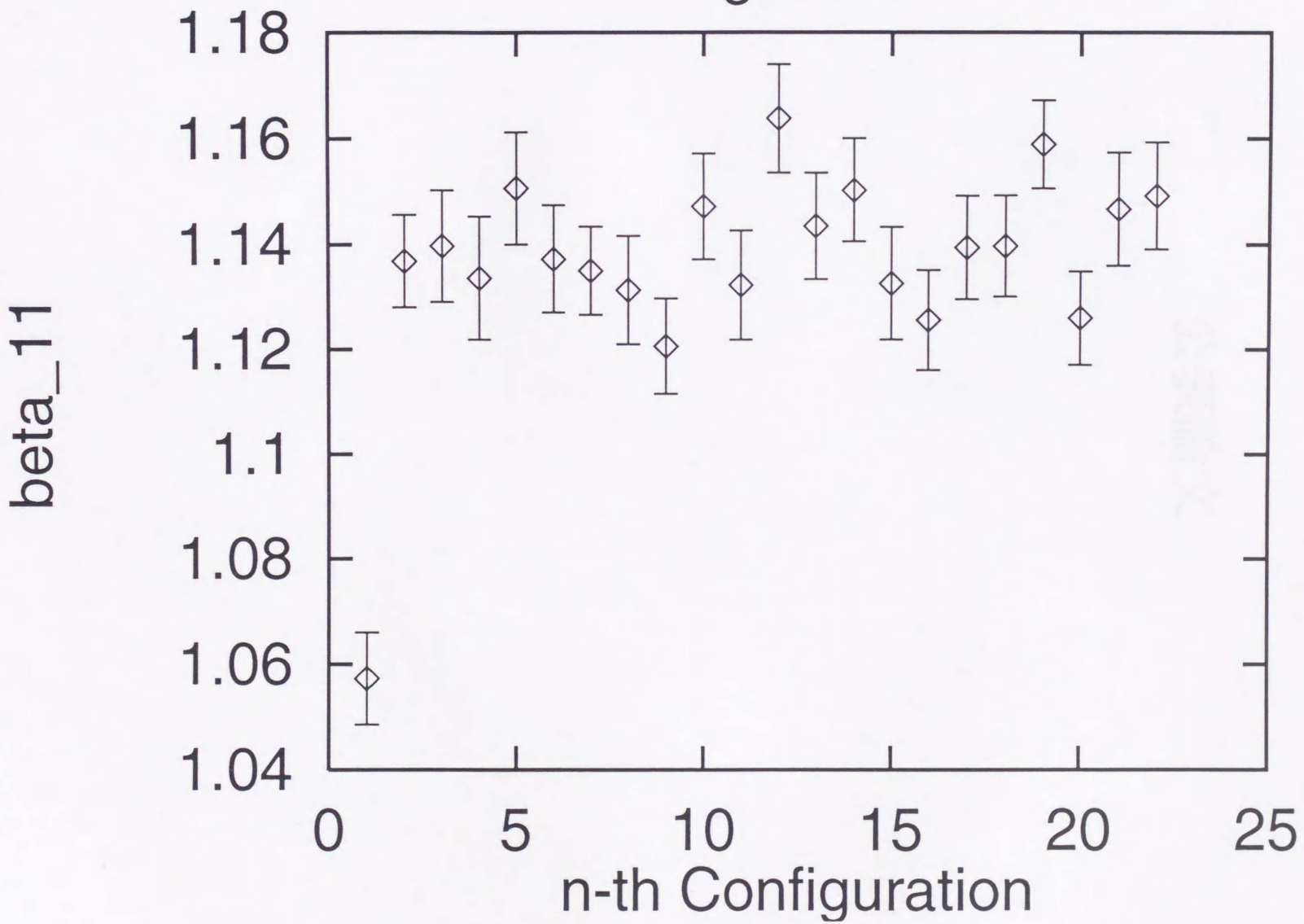
1.18
1.16
1.14
1.12
1.1
1.08
1.06
1.04
beta_11
0
5
10
15
20
25
n-th Configuration

公表論文

(1) **Scaling study of pure gauge lattice QCD by Monte Carlo renormalization group method**

(共著者) K.Akemi,M.Fujisaki,M.Okuda,Y.Tago,Ph. deForcrand,T.Hashimoto, S.Hioki, O.Miyamura, A.Nakamura and I.O.Stamatescu

（論文誌） Physical Review Letters **71** 3063 (1993)

(2) **Determination of effective actions for SU(3) lattice gauge theory**

（論文誌） Modern Physics Letters A (1995) に掲載決定

参考論文

1 **Bound for the differential cross-section of elastic hadron scattering**

(共著者) M.Kawasaki and T.Ikemoto

(論文誌) Modern Physics Letters A **5** 2599 (1990)

2 **Break structure of forward peaks on elastic pp and anti-p-p scattering at high energies**

(共著者) M.Kawasaki and M.Yonezawa

(論文誌) Physical Review Letteres **67** 1197 (1991)

3 **Generation of shift register random numbers on distributed memory multiprocessors**

(共著者) J.Makino and O.Miyamura

(論文誌) Computer Physics Communications **70** 495 (1992)

4 **Does overrelaxed updating in lattice QCD improve critical slowing down?**

(共著者) K.Akemi,M.Fujisaki,M.Okuda,Y.Tago,Ph. deForcrand,T.Hashimoto, S.Hioki, O.Miyamura, A.Nakamura and I.O.Stamatescu

(論文誌) Physics Letters **B328** 407 (1994)